University of Veterinary Medicine Vienna
Department of Pathobiology
Institute of Microbiology
Head: Univ.- Prof. Dr. Monika Ehling-Schulz

Characterization of virulence factors produced by *Bacillus cereus* involved in sepsis

Master thesis submitted to obtain the academic degree

Master of Science (MSc)

Submitted by

Astrid Digruber, BSc

Vienna, July 2019

Supervisor: Univ. – Prof. Dr. Monika Ehling-Schulz
Institute of Microbiology
Department of Pathobiology
University of Veterinary Medicine Vienna

Co-Supervisor: Markus Kranzler, PhD
Institute of Microbiology
Department of Pathobiology
University of Veterinary Medicine Vienna

Reviewer Dr. Birgit Strobl
Institut für Animal Breeding and Genetics
Department of Biomedical Sciences
University of Veterinary Medicine Vienna

Acknowledgements

First of all, I would like to express my very great appreciation to Univ.-Prof. Dr. Monika Ehling-Schulz for providing me with this great opportunity of writing my Master Thesis about this exciting topic in her lab.

Particularly, I would like to thank Markus Kranzler, PhD, who was a great supervisor for me during my time in the lab, and also for his valuable input and patience during the writing process of my thesis.

Moreover, special thanks go to Tatjana Svoboda for showing me everything I had to know and helped me out in every situation.

I thank all other people in the lab for making my stay unforgettable: Panagiotis Ballas, Eva Maria Kalbhenn, Susanna Leiter, Katharina Mayer, Stelli Stancheva, Stefanie Strobl, Marlene Heugl, Valerie Wagner, Helene Marbach, Tom Grunert and Agnieszka Gacek-Matthews. It was always a pleasure coming to work!

Also, I would like to express my gratitude to Dr. Birgit Strobl and Mag. Andrea Pölzl (Institute for Animal Breeding) for providing bone-marrow-derived macrophages and supporting me during my experiments.

My sincere thanks also go to Mag. Waldtraud Tschulenk and Ao. Univ.-Prof. Dr. Ingrid Walter (Institute of Pathology) for their valuable input and their enthusiasm while working with my samples.

Furthermore, I would like to thank Dr. Katharina Nöbauer, Dr. Karin Hummel, Mag. Sarah Schlosser and Ao. Univ.-Prof. Dr. Ebrahim Razzazi-Fazeli (VetCore, Core Facility for Research) for performing mass spectrometry.

I also thank Maximilian Mayerhofer and Christoph Metzner for various scientific discussions and their input.

Last but not least, I thank my family and friends for their support. Without them I would not be where I am today.

“I declare on my word of honour that I have written this paper on my own and that I have not used any sources or resources other than stated and that I have marked those passages and/or ideas that were either verbally or textually extracted from sources. This also applies to drawings, sketches, graphic representations as well as to sources from the internet.
The paper has not been submitted in this or similar form for assessment at any other domestic or foreign post-secondary educational institution and has not been published elsewhere.”

Table of contents

1. Introduction

1.1. The *Bacillus cereus* group

The genus *Bacillus* belongs to the family Bacillaceae, which comprise Gram-positive, rod-shaped, heterotrophic bacteria, which have the ability to produce endospores (Ehling-Schulz *et al*., 2011; Ehling-Schulz & Messelhäusser, 2014) . Most Bacillaceae are non-pathogenic, and are either obligate aerobes or facultative anaerobes (Claus & Fritze, 1989). In 1887, Frankland & Frankland isolated the first *Bacillus cereus* strain in a cow shed (Frankland & Frankland, 1887). Since then, *B. cereus* is found widely spread in nature. *B. cereus* is part of *Bacillus cereus sensu lato*, which consists of six species: *Bacillus cereus sensu stricto*, *Bacillus mycoides*, *Bacillus pseudomycoides*, *Bacillus thuringiensis*, *Bacillus weihenstephanensis* and *Bacillus anthracis* (Stenfors Arnesen *et al*., 2008). However, this grouping is controversial, as the species are mainly differentiated mainly by their morphological and pathological appearance, but not by their genetic distances. For instance, the 16S rDNA sequence is shared by 99 % of *B. anthracis, B. cereus* and *B. thuringiensis* strains (Ash *et al.,* 1991*).* Considering chromosomal markers, *B. cereus* and *B. thuringiensis* cannot be distinguished as two different species (see for review Helgason *et al*., 2000). Furthermore, emetic *B. cereus*, which share their pCER270 plasmid backbone to that of *B. anthracis* pXO1, show a closer relationship to *B. anthracis* than to non-emetic *B. cereus* strains (Ehling-Schulz *et al*., 2006; E Helgason *et al*., 2004; Keim *et al*., 2000). Hence, the presence or absence of plasmids or other morphological or physiological traits distinguish these species from each other (Auwera *et al*., 2007). *B. thuringiensis* is commonly used in agriculture to protect crops from insects, as it produces insecticidal endotoxins during sporulation (Aronson & Shai, 2001). *B. anthracis* is the causative agent of the anthrax disease and is known for its use as a biological weapon (Jernigan *et al*., 2002). It is primarily differentiated from *B. cereus* by the presence of two plasmids, pXO1 (182 kb) and pXO2 (95 kb) (Kolstø *et al*., 2009). These plasmids contribute mainly to the virulence of *B. anthracis*. The anthrax toxin genes encoding for the protective antigen, lethal factor and edema factor are located on pXO1, while the genes encoding for capsule synthesis are located on pXO2 (for review see Mock & Fouet, 2001). *B. mycoides* and *B. pseudomycoides* can be differentiated from *B. cereus* only by their shape and fatty acid content (Nakamura & Jackson, 1995). Formerly, *B. cereus* was classified as a mesophilic microorganism, with a growth range of 10 °C - 50 °C and an optimal growth rate between 35 °C - 50 °C (Claus & Fritze, 1989). Though, in the last decades an increasing number of psychrotolerant *B. cereus* strains were reported. Consequently, a new species within the group was established, termed *B. weihenstephanensis*. This species has the ability to grow below 7 °C, but not at

43 °C anymore. Another characteristic of *B. weihenstephanensis*, is a specific 16S rDNA sequence and a signature sequence in the cold-shock protein gene *cspA* (Lechner *et al*., 1998).

In the last decade, two species were attributed to the *Bacillus cereus sensu lato group*, namely *B. cytotoxicus* and *B. tyoyonensis* The first strain, isolated during a fatal food-poisoning outbreak in France, is a thermotolerant strain and therefore grows at temperatures up to 50 °C, the latter is used as a probioticum (Guinebretiere *et al*., 2013; Jiménez et al., 2013).

1.2. Pathogenic potential of *Bacillus cereus*

Due to its environmental ubiquitous presence, *B. cereus* is also found in a wide range of dried foods, for example rice and spices, but also in dairy products and vegetables (Kramer & Gilbert, 1989). In addition, spores can also lead to affected meat products (Stenfors Arnesen *et al*., 2008). The diseases, which are caused by *B. cereus,* affect the gastrointestinal tract (GI tract) and are characterized by either the emetic or the diarrhoeal syndrome. The contributing agents of these two distinct syndromes are exotoxins that are produced by certain *B. cereus* strains. Each of these diseases is based on a different etiologic mechanism (for review see Ehling-Schulz *et al*., 2019).

The pathogenic agents of the diarrhoeal syndrome are the non-haemolytic enterotoxin (Nhe), haemolysin BL (Hbl) and cytotoxin K (CytK) (Beecher & MacMillan, 1991; Lund *et al*., 2000; Lund & Granum, 1996). The gene profile of the three enterotoxins is versatile amongst various strains. Genes encoding for Nhe are present in all *B. cereus* strains, whereas Hbl and CytK are only present in up to 50% of randomly sampled strains (Moravek et al., 2006). The onset of food poisoning-related symptoms evoked by the enterotoxins takes 8 to 16 h, and normally lasts not longer than 24 h. Foods containing high amounts of protein, for example meat products, soups and vegetables, are often the source of this type of disease (for review see Ehling-Schulz *et al*., 2011; Stenfors Arnesen *et al*., 2008).

The emetic disease is caused by cereulide, a small, cyclic, heat-stable dodecadepsipeptide, which is formed by a small percentage of *B. cereus* strains and can be found predominantly in foods rich in starch, for example rice, pasta and pastries, but also infant and convenience food (Ehling-Schulz *et al*., 2004). Due to the resistance against heat, acids and proteases, neither reheating of foods nor gastric acids and proteolytic enzymes of the GI tract can degrade the peptide. Also, filtration is not applicable due its small size of 1.2 kDa. (Agata *et al*., 2002; 1961). Cereulide intoxication is characterized by a fast onset (30 min to six hours) however, these diseases are usually self-limiting and normally last no longer than one day. Food poisoning after intake of *B. cereus* toxins, that required hospitalization or with fatal outcome, are rare but reported. In 2008, a 20-year old man died after eating spaghetti stored

for 5 days at room temperature (Naranjo *et al*., 2011). Five years earlier, a similar case happened, at which a family consumed pasta salad, prepared three days prior consumption and insufficiently cooled in the fridge (Dierick *et al*., 2005).

During the last decades, *B. cereus* is also gaining importance as a human pathogen provoking various non-GI related diseases, including endocarditis, septicaemia, gas gangrene-like infections and cutaneous infections (Bottone, 2010; Messelhäußer & Ehling-Schulz, 2018; Oda *et al*., 2012).

Nosocomial *B. cereus* outbreaks mostly occur in immune compromised patients, in which contaminated hospital linen or inaccurate maintenance of central venous catheters lead to *B. cereus* infections (Dohmae *et al*., 2008). Hence it is also crucial to correctly identify *B. cereus* in skin lesions and wounds of immune competent as well as in immune compromised individuals. Misidentification with *Clostridium perfringens* and treatment with penicillin, leads to a severe damage and to a delay of recovery, due to the intrinsic resistance of *B. cereus* against penicillin (Bottone, 2010). The virulence factors inducing non GI-related diseases caused by B. cereus are so far unknown. Hence, secreted factors have been discussed recently, which will be shortly described in the following sections.

1.2.1. Non-haemolytic enterotoxin

Nhe is a pore-forming enterotoxin, consisting of the three components NheA, NheB and NheC. NheA is the largest subunit of Nhe with 41.09 kDa, followed by NheB with 39.82 kDa and NheC with 36.48 kDa (Granum *et al*., 1999).

The three Nhe subunits have to bind in a specific order and in a specific ratio for maximal cytotoxicity. It was shown that a ratio of NheA:NheB:NheC = 10:10:1 is most effective, however, an increase of NheC resulted in a decrease of toxic activity by binding to NheB and following inhibition of the Nhe pore complex formation (Lindbäck *et al*., 2004, 2010). The cytotoxic effect of Nhe is based on direct pore formation, and – so far – no inflammasome-mediated mechanism was shown (Fagerlund *et al*., 2008).

Expression of Nhe is mainly regulated by the phospholipase C regulator (PlcR) quorum-sensing system (Ravnum *et al*., 2008). PlcR is activated by a small peptide, PapR, which accumulates inside the bacterial cell when high bacterial cell densities are reached (Slamti & Lereclus, 2002). Disruption of *papR* resulted in decreased expression of PlcR, leading to decreased hemolysis and virulence in *vivo* and in *vitro* (Salamitou *et al*., 2000).

1.2.2. *Bacillus cereus* sphingomyelinase

Sphingomyelinase (SMase) belongs to the group of phospholipases C, and is an enzyme widely distributed in Gram-negative and Gram-positive bacteria (Flores-Díaz *et al*., 2016). Two different types of SMases can be differentiated: SMase C, which cleaves sphingomyelin

to ceramide and phosphorylcholine and SMase D, which cleaves sphingomyelin to Cer-1-phosphate and choline (for review see Flores-Díaz *et al*., 2016). Ceramide, released by SMase C cleavage, acts as a signalling molecule and is able to induce cell lysis, cell cycle arrest and apoptosis. It was also shown that autophagy and cytokine production is influenced by this molecule (Kolesnick & Golde, 1994). Cer-1-phosphate, released by Smase D cleavage, acts similar to ceramide as a signalling molecule, but stimulates cytoxolic phospholipase A2, as well as macrophage chemotaxis, cell proliferation and inflammation (for review see Go, 2004)

The SMase of *Bacillus cereus* belongs to the first SMase type and is classified as a metal ion-dependent phospholipase, hydrolysing sphingomyelin to phosphorylcholine and ceramide and further leading to host cell lysis by affecting its membrane integrity (Ago *et al*., 2006). It is suggested that SMase is a key virulence factor, as it acts synergistically with Nhe and Hbl, thereby enhancing the toxic potential (Beecher *et al*., 2000; Doll *et al*., 2013). It was also shown that SMase is able to bind ganglioside GM3 or GM3-like structures on cell membranes and to downregulate phagocytic activity of macrophages (Oda *et al*., 2013, 2012). Accordingly, SMase was able to induce lethality in mice, contrary to other phospholipases (Oda *et al*., 2012). In addition, high levels of ceramide and phosphorylcholine were shown to correlate with sepsis mortality (Drobnik *et al*., 2003). Structurally, SMase shares similarities to the *Staphylococcus aureus* beta toxin, *Clostridium perfringens* alpha toxin and the *Listeria ivanovii* sphingomyelinase (Ago *et al*., 2006; Gilmore *et al*., 1989; Openshaw *et al*., 2005).

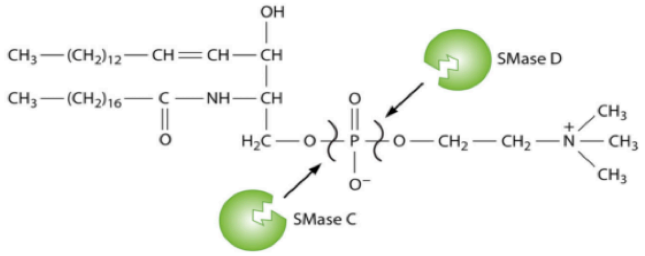

Figure 1: Schematic illustration of SMase cleavage sites Adapted from (Flores-Díaz *et al*., 2016).

1.2.3. Other Phospholipases

According to their substrate specificity, three types can be distinguished: phosphatidylinositol-specific phospholipase C (PI-PLC) and phosphatidylcholine-specific phospholipase C (PC-PLC) and the before mentioned SMase. Along with SMase, these phospholipases cleave glycerophospholipids of eukaryotic and prokaryotic membranes, specific to their substrate sphingomyelin, phosphatidylinositol or phosphatidylcholine, which finally results in pore formation and cell lysis (Slein & Logan, 1965; Titball, 1993). PI-PLC is expressed in a similar manner by *B. cereus*, B*. thuringiensis* and *B. anthracis*, with 94 % amino acid identity amongst the species (Pomerantsev et al., 2003; Read et al., 2003).

Studies showed that PI-PLC cleaves glycosylphosphatidylinositol-anchored proteins (GPI-anchored proteins), which are crucial for dendritic cell activation (Sharom & Lehto, 2002). Insufficiently activated dendritic cells, result in diminished expression of the co-stimulatory molecule CD86 (Zenewicz *et al*., 2005).

In contrast to PI-PLC, PC-PLC also recognizes – in addition to phosphatidylcholine (PC) – phosphatidylethanolamine (PA) and phosphatidylserine (PS), however, its highest specificity is shown towards PC (Martin *et al*., 2000). The *B. cereus* PC-PLC is identical to the *B. thuringiensis* PC-PLC, both enzymes are able to hydrolyse sheep erythrocytes. Though, the synergistic effect of PC-PLC and SMase also enables to lyse human erythrocytes. However, the synergy of both enzymes is also termed “cereolysin AB” as both toxins are encoded as an operon (Gilmore *et al*., 1989). The unusual proportions of phospholipids in retinal tissue can explain the severity of *B. cereus*-induced endophalmitis. All three substrates cleaved by PC-PLC were found in this tissue. However, sphingomyelin, which was shown to inhibit PC-PLC activity, was only present in low levels (Alonso *et al*., 1998; Berman, 1991).

1.2.4. Other Virulence factors

Collagenase

Several collagenases have been described so far, and been either classified as “true” collagenases or pseudo-collagenases. The latter degrade gelatin, or non-helical sections of collagen, while “true” collagenases are able to cleave triple-helical regions (Harrington, 1996). Bacterial collagenases, secreted by *Borrelia burgdorferi* and *C. perfringes,* for example, are classified as true collagenases (Grab & Philipp, 1996; Matsushita *et al*., 1994).

However, degradation of collagen has severe consequences for the host, as collagen is one of the major components of the extracellular matrix (ECM) in vertebrates. The major components of the ECM can be grouped into two classes: Fibrous proteins, which are next to collagen, elastin, fibronectin and laminin, and proteoglycans, which fill the interstitial space composed of fibrous proteins (Järveläinen *et al*., 2009; Schaefer & Schaefer, 2010; see for review Theocharis *et al*., 2015). The ECM is not only fundamental to provide physical support, moreover, it is also involved in several processes, for example, growth, differentiation and morphogenesis (see for review Theocharis *et al*., 2015).

However, *B. cereus* harbours a collagenase with a size of 105 kDa (Abfalter *et al*., 2016; Lund & Granum, 1999). It is a $Ca2^{+}$ and $Zn2^{+}$ dependent metalloprotease that is able to digest native collagen at room temperature and at physiological pH (Sela *et al*., 1998). Regarding to its toxic potential, this enzyme is considered as an important virulence factor in *B. cereus* endophalmitis (Beecher *et al*., 2000).

Flagella

The flagellum is a bacterial structure, enabling movement. Depending on the environment, it can either direct the organism towards favourable or escape from unfavourable conditions (Wang *et al*., 2005). The *B. cereus* flagellum is anchored in the cytoplasm and reaches into the environment. Many diverse arrangements, for example monotrichous and petritrichous flagellation, and its assembly of more than 30 different proteins undermine the complex structure (Macnab, 1992; Wolffian & Conn, 1938). Flagellin is the most prominent protein of the flagellum, as it forms the flagellar filament. It is synthesised in the cytoplasm and transferred through the cell membrane to the bacterial cell surface. At the bacterial cell surface, it finally assembles to its final filamental structure (Macnab, 1992). In addition to its important feature as a locomotion unit for bacteria, it stimulates the innate immune system as it is detected by Toll like receptor 5 (TLR-5, Hayashi *et al*., 2001). TLR5-response to flagellin activates myeloid differentiation primary response 88 (MyD88)-dependent signalling, and induces the activation of nuclear factor kappa-light-chain-enhancer of activated B-cells (NF-κB), leading to activation of innate immune responses against the flagellated pathogen (Gewirtz *et al*., 2001). Moreover, there is a clear link between the pathogenicity, motility and flagellation, as *B. cereus* mutants lacking the protein to enable swarming, also were less cytotoxic (Mazzantini *et al*., 2016).

1.3. Extracellular vesicles and their pathogenic potential

Extracellular vesicles (EVs) are structures consisting of lipid-bilayers that form lumen-containing spheres, with a diameter size from 20 nm to 500 nm that are not able to replicate (Deatheragea & Cooksona, 2012). The release of such structures seems to be preserved among all domains. The most extensively studied EVs are those released from mammalian cells. These EVs seem to be have crucial roles for instance in autophagy, cancer and as biomarkers (Birnbaum *et al*., 2019; Hessvik *et al*., 2016; Katsu *et al*., 2019). EV release was also shown for all other kingdoms. Therefore a broad range the broad range from Gram-negative and Gram-positive bacteria to archaea, and multicellular organisms, such as parasites, fungi and plants (Ellen *et al*., 2009; Mcbroom *et al*., 2006; Oliveira *et al*., 2010; Rivera *et al*., 2010; Rutter & Innes, 2017; Silverman *et al*., 2010). So far, lacking secretion of extracellular vesicles was demonstrated only in Chromista (Ruggiero *et al*., 2015).

Since the 1970s, rare observations of fungal or bacterial extracellular vesicles have been reported (Takeo *et al*., 1973; Work *et al*., 1966). The existence of EVs derived from Gram-positive bacteria was first reported in 1990 (Dorward & Garon, 1990). Although EV research is progressing, it remains still unclear how extracellular vesicles escape thick cell walls of Gram-positive bacteria, mycobacteria and fungi. During the last decades, several Gram-positive bacteria and fungi that produce EVs have been observed, for example in

Staphylococcus aureus, *Mycobacterium tuberculosis, B. anthracis* and *Cryptococcus neoformans* (J. Lee *et al*., 2015; Rivera *et al*., 2010; Rodrigues et al., 2008; Schlatterer *et al*., 2018). Using various microscopic scanning methods, like transmission electron micrography (TEM) or atomic force microscopy (AFM), bacterial blebbing of extracellular vesicles has been observed (Dean *et al*., 2019; Deatheragea & Cooksona, 2012).

EVs originating from *B. anthracis* were shown to contain the three anthrax toxin components protective antigen, lethal factor and endema factor, as well as other proteins relevant for stress responses and metabolism (Rivera *et al*., 2010). Also *Bacillus subtilis,* a non-pathogenic species belonging to the genus *Bacillus,* was shown to produce such structures (Brown *et al*., 2014). So far, valid data on secretion and function of EVs and its putative toxin content are still missing for *B. cereus*. In regard to pathogenicity, EVs of *Bacillus cereus* are crucial to contemplate, as the secretion of extracellular vesicles might contribute to its pathogenicity in a yet unknown manner.

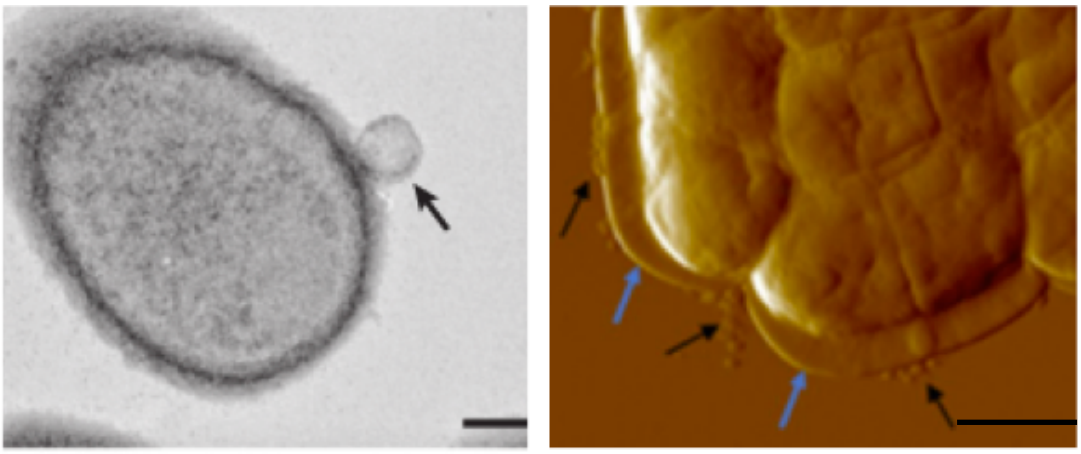

Figure 2: TEM Image of *Listeria monocytogenes* EV (a) and AFM Image of *Lactobacillus reuteri* EVs (b). Black arrows indicate EVs; Scale bar represents 100 nm and 600 nm, respectively (Brown *et al*., 2014; Dean *et al*., 2019).

1.3.1. MISEV guidelines

In order to ensure standardization, guidelines on minimal information for studies of extracellular vesicles (MISEV) were established. In 2014, the first guidelines (MISEV 2014) were published as a position editorial, and four years later, the sequel MISEV 2018 was published (Théry *et al*., 2018). These guidelines describe experimental settings and controls, which should be considered in terms describing extracellular vesicles and their functions. EVs research in mammals and humans is far more advanced than in prokaryotes. Along with progressing research, various terms for EVs have been established, such as microvesicle or exosome (Gould, 2013). However, the international society for extracellular vesicles (ISEV) recommends “extracellular vesicle” (EV) as the common name for particles fulfilling the above mentioned criteria (lipid-bilayer, not able to replicate) (Théry *et al*., 2018).

To classify EVs more precisely, terms describing physical properties, such as EV size or cell origin, should be used. Current classification for EV sizes are as following: Small EVs <100 nm (sEVs), medium EVs 100-200 nm (mEVs), large EVs >200 nm (lEVs) (Théry et al., 2018). Accordingly, guidelines have been established to provide a framework for standardized classification and experimental procedures (Théry et al., 2018)

1.3.2. EVs in Gram-negative bacteria

The Gram-negative cell wall consists of an outer membrane and an inner membrane, which differ in lipid and protein composition. The outer leaflet of the outer membrane is dominantly composed of a lipopolysaccharide (LPS), whereas the inner leaflet and membrane consists of phospholipids (Bos *et al*., 2007). LPS is released when the outer membrane gets degraded or destroyed, and acts as an endotoxin. Since LPS, which is structurally comparable with ceramide, binds to CD14 – a receptor found on many cell types including monocytes, dendritic cells, macrophages and B-cells – proinflammatory cytokines are released (Wright & Kolesnick, 1995). Leading to extensive release of cytokines, possibly resulting in septic shock with fatal outcome (Yamamoto *et al*., 2019).

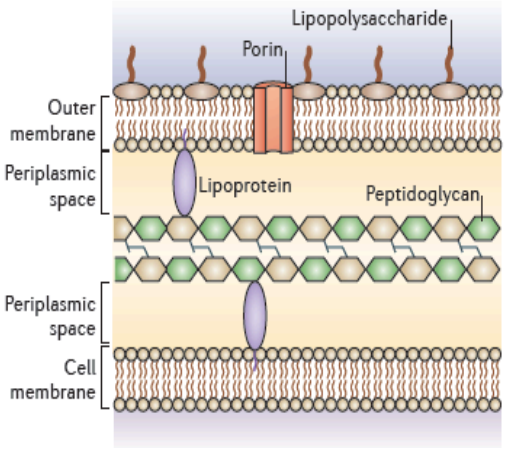

Figure 3: Cell wall structure of Gram-negative bacteria (Brown *et al*., 2015).

These two membranes confine the periplasmic space, which has a viscous consistency, and makes up to 7 – 40 % of the total cell volume. Throughout the periplasmic space, a thin peptidoglycan layer connects the outer and inner membrane by membrane-anchored proteins such as murein lipoprotein (Lpp) and OmpA (for review see Kulp & Kuehn, 2010). Important proteins located in the outer membrane, such as envelope stressors, are involved in sensing environmental stressors and are able to repair damage (Raivio, 2005).

Vesicles of Gram-negative bacteria, called outer-membrane vesicles (OMVs), consist mainly of phospholipids, outer membrane proteins, and lipopolysaccharides. Periplasmic proteins and trapped cell wall components were found in the particle lumen (Roier *et al*., 2015). Though, OMVs also include inner membrane proteins, cytoplasmic proteins, DNA, RNA, ions, metabolites and signalling molecules (Altindis *et al*., 2014; Bitto *et al*., 2017; Koeppen *et al*., 2016; Sjöström *et al*., 2015)

OMVs are considered to have crucial roles not only in bacterial physiology, but also in pathogenesis. Studies suggest involvement in horizontal gene transfer, biofilm formation, intra-interspecies communication, stress response, delivery of toxins, killing of competing microbial cells, antibiotic resistance, host adherence and immunomodulation. Consequently,

also vaccines containing vesicles constitute promising candidates to combat bacterial infections (for review see Toyofuku *et al*., 2019).

A current hypothesis of OMV formation in Gram-negative bacteria is based on the fact that phospholipids accumulate in the outer membrane due to decreased or altered gene expression. This swelling leads to budding of the outer membrane, due to phospholipids inducing positive and negative curvature. Finally, the OMV gets released, supplemented with the inserted phospholipids (Roier *et al*., 2015). However, this hypothesis does not exclude other theories of vesicle formation, suggested so far. In addition, species-specific OMV formation and differences have to be considered (Wang *et al*., 2018).

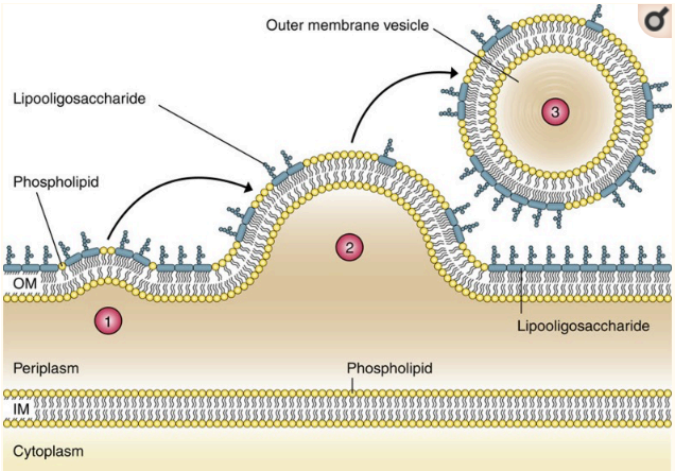

Figure 4: Illustration of vesiculogenesis in gram-negative bacteria (Roier *et al*., 2015)

1.3.3. EVs in Gram-positive bacteria

In contrast to Gram-negative bacteria, Gram-positive bacteria have one single lipid membrane that is surrounded by a thick cell wall composed of peptidoglycan. The peptidoglycan layer forms a linear glycan strand due to disaccharide-peptide repeats combined with glycosidic bonds and form a mesh-like structure. The peptidoglycan wall is 30 – 100 nm thick and crucial to provide structural stabilization and protection from the environment (Silhavy *et al*., 2010).

Within this layer, a number of proteins such as teichoic acids (an anionic polymer) are anchored. These can be divided into two classes: wall teichoic acids (WTAs), which are anchored to peptidoglycan, and lipoteichoic acids (LTAs), which are bound to the cell membrane. In combination, WTAs and LTAs are important to bind cations and therefore ensure a steady cation homeostasis. Metal cations and WTAs also influence the structure and robustness of the cell wall (Neuhaus & Baddiley, 2003).

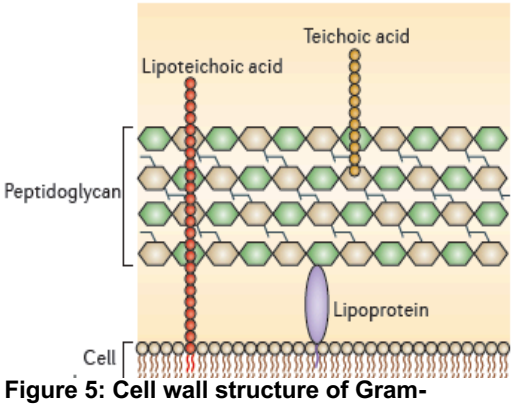

Figure 5: Cell wall structure of Gram-positive bacteria (Brown *et al*., 2015).

Protein composition of extracellular vesicles (EVs) secreted by *Staphylococcus aureus* was described by mass spectrometry in 2009 (Lee *et al*., 2009). The EV sizes were found to be 20 – 100 nm in diameter, which can be compared to OMVs isolated from Gram-negative bacteria. Their content included a number of proteins that are important for survival and virulence (Lee *et al*., 2009)

Various EV sizes secreted by Gram-positive bacteria were described. Characterisation of *B. subtilis* EVs showed a very heterogeneous EV population, suggesting the existence of a cargo-sorting machinery (Brown *et al*., 2014). EVs from *Staphylococcus spp*., and *L. monocytogenes* were found to be in a range from 20 to 150 nm in diameter, whereas EVs from Bacillus *spp*., *C. perfringens* and *Streptomyces coelicolor* are found to cover a broader diameter range (20 to 400 nm in diameter, Brown *et al*., 2014; Lee *et al*., 2009; Rivera *et al*., 2010; Schrempf *et al*., 2011; Yanlong *et al*., 2014). Although vesiculogenesis appears as a general mechanism, the process of formation is species-dependent and needs further investigation.

Three hypotheses on the mechanism of vesicle release in Gram-positive bacteria are currently proposed. EVs may be released through turgor pressure, which pushes the vesicle through the wall. Release of EVs might also be

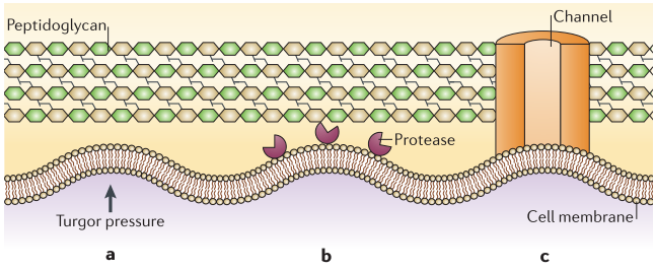

Figure 6: Hypothesis of vesiculogenesis in Gram-positive bacteria (Brown *et al*., 2015)

regulated by pore size or thickness (Rodrigues et al., 2008). Alternatively, cell wall modifying enzymes, for example proteases, could facilitate the permeability of the cell wall (Albuquerque *et al*., 2008). It has been shown that *S. aureus* possesses an enzyme called Sle1 that is able to degrade peptidoglycan. EV might also migrate through pores or channels, due to the ability to modify their structure (Rodrigues *et al.*, 2008; Vallejo *et al*., 2012).

1.3.4. Pathogenic potential of EVs

Even though vesiculogenesis is not fully understood yet, the pathogenic potential of EVs is widely accepted. In *C. perfringens,* EVs were shown to transport chromosomal DNA encoding for toxins. However, *C. perfringens* EVs were not toxic to macrophages, probably due to the lack of perfringolysin O (PFO) in these EVs or lacking transcription of the toxin-encoding genes. Nevertheless, *in vitro* experiments initiated the production of inflammatory cytokines such as tumour-necrosis factor (TNF), interleukin-6 (IL-6) and granulocyte colony stimulating factor (GCSF, Yanlong *et al*., 2014).

It was also shown that bacterial EVs interfere with host cells and can stimulate the host's immune responses. *S. aureus* EVs were capable to upregulate pro-inflammatory mediators *in vitro* and *in vivo*. In tape-stripped mice, EVs caused a T-helper 17 (TH_{17}) response and increased production of immunoglobulin E (IgE), causing atopic dermatitis-like inflammation (Hong *et al*., 2011). Correspondingly, disruption of EVs promotes the ability of lipoproteins to activate toll-like receptor 2 (TLR2, Schlatterer *et al*., 2018). In *B. anthracis,* toxin-containing extracellular vesicles deliver the contents after fusion with cholesterol microdomains directly into the host cell (Rivera *et al*., 2010). Also, EVs of mycobacterial origin are able to modulate the immune response. TLR1 and TLR2 recognize mycobacterial EV ligands, leading to activation of NF-κB and mitogen-activated protein kinase (MAPK) pathways. Further, this results in an increase of the immune response and a decrease of antigen presentation (Prados-Rosales *et al*., 2011).

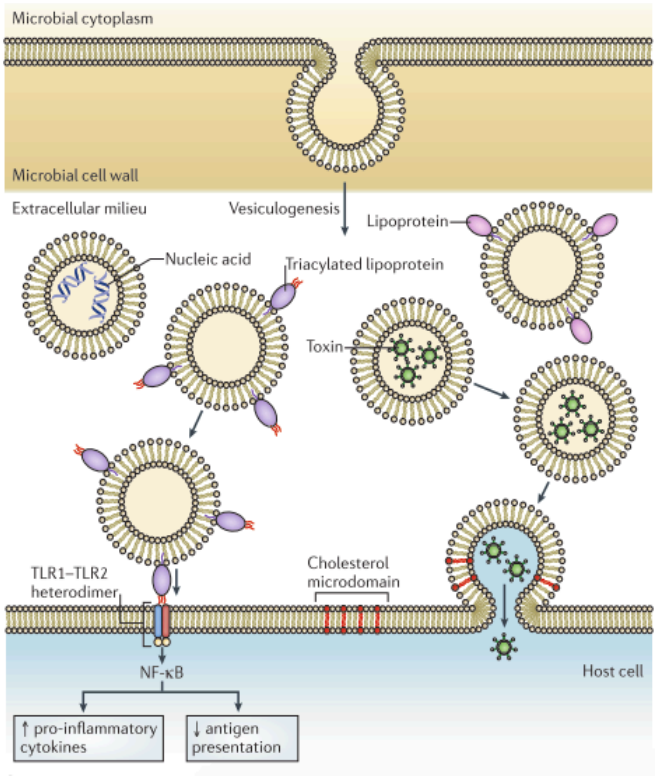

Figure 7: Pathogenic potential of EVs (Brown *et al*., 2015).

1.4. Study aim

The main aim of this thesis is the characterisation of extracellular vesicles released by *Bacillus cereus* and the assessment of potential pathogenic properties of EVs, which may contribute to non GI-related systemic diseases caused by *B. cereus*

The first objective was therefore to establish a protocol to purify extracellular vesicles from the bacterial main culture. Then a proteomic and western blot approach was used to detect already well-studied *B. cereus* toxins in the extracellular structures. Also, EV production was compared between standard laboratory and simulated intestinal conditions. Transmission electron microscopy was used, to obtain images of *B. cereus* EVs and evaluate their sizes, as suggested by the MISEV guidelines. In order to study their pathogenic potential, a cell culture was established, using murine bone marrow derived macrophages (BMDMs). These cells are frequently used to study sepsis and the impact of pathogens (Bosmann *et al*., 2014; Oda *et al*., 2013).

2. Materials & Methods

2.1. Buffer receipts in alphabetical order

10x Blotting buffer

- 500 mM Tris (Carl Roth, Germany)
- 390 mM Glycin (Carl Roth, Germany)
- 0.039 % sodium dodecyl sulfate (Carl Roth, Germany)
- MQ-H_2O (Merck Millipore, USA) ad 1000 ml

1x Blotting buffer (500mL)

- 50 ml 10x Blotting Puffer
- 50 ml Methanol (Carl Roth, Germany)
- MQ-H_2O (Merck Millipore, USA) ad 500 ml

Destaining olution

- 40 ml MeOH (Carl Roth, Germany)
- 15 ml Acetic acid (Carl Roth, Germany)
- MQ-H_2O (Merck Millipore, USA) ad 200 ml

Fixing solution

- 25 % Isopropanol (Carl Roth, Germany)
- 10 % Acetic acid (Carl Roth, Germany)
- MQ-H_2O (Merck Millipore, USA) ad 50 ml

4x Laemmli (20mL)

- 8 % SDS (Carl Roth, Germany)
- 40 % Glycerol (Carl Roth, Germany)
- 250 mM Tris-HCl pH 6.8 (Carl Roth, Germany)
- MQ-H_2O (Merck Millipore, USA) ad 20 ml
- Add Bromphenolblue (Carl Roth, Germany) till the buffer is dark blue
- 100 mM dithiothreitol (DTT, Carl Roth, Germany)
- Add prior to use: 20 µl 3M DTT (Carl Roth, Germany) to 120 µl 4x Laemmli

Lysis buffer

- *2x Schindlers Buffer*
- *3 M NaCl (*Carl Roth, Germany)
- *1 M DTT* (Roche, Switzerland)
- *100 mM Na-vanadate* (Sigma-Aldrich, USA)
- *500 mM Na-flouride* (Sigma-Aldrich, USA)
- *100 mM phenylmethylsulfonyl fluoride* (PMSF, Sigma-Aldrich, USA)
- *100* µg/µl Leupeptin (Sigma-Aldrich, USA)
- *100* µg/µl Aprotinin (Sigma-Aldrich, USA)
- *100* µg/µl Pepstatin (Sigma-Aldrich, USA)
- fill up with MQ-H_2O (Merck Millipore, USA)

10x pyTris-buffered saline (pyTBS)

- 10 mM Tris pH 7.4
- 75 mM NaCl

- 1 mM EDTA pH 8
- MQ-H_2O (Merck Millipore, USA) ad 1000 ml

1x pyTris-buffered saline with tween (pyTBS-T)

- 100 ml 10x pyTBS
- 0.1% Tween 20 (Carl Roth, Germany)

10x Tris-buffered saline (TBS)

- 0.2 M Tris (Carl Roth, Germany)
- 1.5 M NaCl (Carl Roth, Germany)
- MQ-H_2O (Merck Millipore, USA) ad 1000 ml

1x Tris-buffered saline with tween (TBS-T)

- 100 ml 10x TBS
- 0.1 % Tween 20 (Carl Roth, Germany)
- MQ-H_2O (Merck Millipore, USA) ad 1000 ml

5x milk powder in TBS-T/pyTBS-T

- 2.5 g milk powder (Carl Roth, Germany)
- 1x TBS-T/pyTBST ad 50 mL

1x milk powder in TBS-T or pyTBS-T

- 0.5 g milk powder (Carl Roth, Germany)
- 1x TBS-T or 1x pyTBST ad 50 mL

10x Running buffer

- 250 M Tris (Carl Roth, Germany)
- 1.92 M Glycin (Carl Roth, Germany)
- 1 % SDS (Carl Roth, Germany)
- MQ-H_2O (Merck Millipore, USA) ad 1000 ml

1x Running buffer

- 100 ml 10x Running buffer
- MQ-H_2O (Merck Millipore, USA) ad 1000 ml

2x Schindler's Buffer

- 1 % octylphenoxypolyethoxyethanol (Sigma-Aldrich, USA)
- 10 % 1 M Tris-Hcl (Sigma-Aldrich, USA)
- 5 % Glycerol (Sigma-Aldrich, USA)
- 2.5 % 0.5 M EDTA (Sigma-Aldrich, USA)
- MQ-H_2O (Merck Millipore, USA)

Stripping Buffer

- 2 M Glycin pH 2,5 (Carl Roth, Germany)
- 0.25 % SDS (Sigma-Aldrich, USA)
- MQ-H_2O (Merck Millipore, USA) ad 1000 ml

2.2. Bacteria and media

2.2.1. Bacillus cereus strains

The enteropathogenic *Bacillus cereus* strains BC25 and its isogenic mutants (*ΔnheBC, Δsph, ΔnheBCΔsph*), BC1 and its isogenic mutant (*ΔplcR*) were used for isolation of extracellularly secreted vesicles for further analysis. Additional information about the strains is given in the table below (table 1).

Table 1: Overview *of Bacillus cereus* strains and isogenic mutants.

Annotation	Official Annotation	Source	Origin	Sent by/Source
BC1	ATCC14579	soil	USA	DSM
BC25	NVH 0075-95	stew with vegetables, foodpoisoning	Norway	(Lund & Granum, 1996)
BC25*ΔnheBC*	NVH0075-95*ΔnheBC*	Knockout mutant of NVH 0075-95	Norway	(Fagerlund *et al*., 2008)
BC25*Δsph*	NVH0075-95*Δsph*	Knockout mutant of NVH 0075-95	Germany	(Doll *et al*., 2013)
BC25*ΔnheBCΔsph*	NVH0075-95*ΔnheBCΔsph*	Knockout mutant of NVH 0075-95	Germany	(Doll *et al*., 2013)
BC1*ΔplcR*	ATCC14579*ΔplcR*	Knockout mutant of ATCC14579 (Kanamycin resistance)	University of Salzburg	Silja Wessler

2.2.1. Growth media and agar plates

Lysogeny broth (LB broth)

Lysogeny broth was prepared using 10 g/l NaCl (Carl Roth, Germany), 10 g/l Trypton (Oxoid, USA) and 5 g/l yeast extract (Oxoid, USA). The pH of the solution was adjusted to 7.4 +/- 0.2. The solution was then autoclaved for 15 min at 121 °C.

Casein glucose yeast broth (CGY broth)

CGY broth was prepared using 20 g/l casein hydrolysate (Carl Roth, Germany), 6 g/l Yeast extract (Oxoid, USA), 2 g/l ammonium sulphate (Carl Roth, Germany), 14 g/l dipotassium phosphate (Carl Roth, Germany), 6 g/l monopotassium phosphate (Carl Roth, Germany), 1 g/l trisodium citrate dihydrate (Carl Roth, Germany). Substances were mixed and deionized water was added to reach a final volume of 450 ml. The solution was then autoclaved for 15 min at 121 °C. Prior to use, the medium was supplemented with sterile filtered glucose (Carl

Roth, Germany) and magnesium sulphate heptahydrate (Carl Roth, Germany) to reach a final concentration of 1 % and 0.2 % respectively.

Plate count agar (PC agar)

PC agar was prepared using 1 g/l glucose (Carl Roth, Germany), 5 g/l trypton (Oxoid, USA), 2.5 g/l yeast extract (Oxoid, USA) and 15 g/l agar-agar, bacteriological (Carl Roth Germany). Substances were mixed and filled up with deionized water to reach a final volume of 500 ml. The solution was autoclaved for 15 min at 121 °C and cooled down to 45 °C. After reaching the final temperature the solution was poured into petri dishes and air dried for at least 2 h and stored at 4 °C until further use.

Conditioned RPMI medium (cRPMI Medium)

cRPMI Medium was prepared by cultivating Caco-2 cells, a immortalized line of heterogeneous human epithelial colorectal adenocarcinoma cells (Hidalgo et al., 1989), in RPMI 1640 with stable glutamine (Biochrom GmbH, Germany), supplemented with 10% fetal bovine serum (FBS, Sigma-Aldrich, USA). Cells were split every 3 – 4 days until the required amount of flasks was reached, with attention to 90 % confluency. To reach full differentiation of Caco-2 cells, cells were incubated for 14 days. Medium was changed on day 5 and 9. On day 14, medium was discarded and cells were washed twice with 5 ml phosphate-buffered saline (PBS, Sigma-Aldrich, USA). Before harvesting cRPMI, 40 ml RPMI was supplemented with 1 % glucose (Carl Roth, Karlsruhe, Germany) and 2 % casein hydrolysate (Carl Roth, Germany) and incubated for 22 h at 37 °C, 90 % relative humidity (rH) and 7 % CO_2 atmosphere. The next day, the medium was sterile filtered (0.2 µm, Sarsted, Germany), and 40 ml aliquots were frozen at -80 °C until further use.

2.2.2. Bacterial cultivation and isolation of extracellular vesicles

Bacillus cereus strains were routinely cultivated on PC agar plates, BC1*ΔplcR* was maintained on LB agar plates supplemented with 250 µg/ml Kanamycin. Under standard conditions, bacteria were pre-cultured for 8 h at 30 °C and 120 rounds per minute (rpm) in 3 ml LB. The main culture was inoculated by adjustment of the pre-culture to OD_{600} = 0.05 in 50 ml LB broth, and grown in 200 ml Erlenmeyer flasks for 2 h, 6 h or 17 h at 30 °C and 120 rpm. To remove bacterial cells, the culture was centrifuged at 3,000 x *g* and 4,000 x *g* for 15 min at 4 °C. Then, the supernatant was sterile filtered (0.2 µm, Sarsted, Germany) and centrifuged at 10,000 x *g* for 15 min at 4 °C. The purified supernatant was condensed from 50 ml to 1 ml using an Amicon ultrafiltration system (100 kDa cut off, Merck Millipore, USA). The concentrated supernatant, containing extracellular vesicles, was collected by ultra-centrifugation at 125,000 x *g* for 1 h at 4 °C (Optima MAX-XP Beckman-Coulter, USA). The resulting pellets were resuspended in 1 ml PBS (Sigma-Aldrich, USA) and centrifuged again.

After this final washing step, the pellets were dissolved in 20 µl PBS (Sigma-Aldrich, USA), and six aliquots were pooled to obtain a total volume of 120 µl vesicle-containing solution.

For incubation in cRPMI, bacteria where first grown in 20 ml CGY medium at 37 °C for 17 h and 120 rpm, before inoculating the main culture by adjusting the pre-culture to OD_{600} = 0.05 in 40 ml of cRPMI. The main culture was incubated in T75 cell culture flasks at 37 °C, 90 % rH, 7 % CO_2 atmosphere for either 2 h, 6 h or 17 h without shaking. Harvesting and all further steps were performed as described for LB.

The protein concentration of the vesicle fraction was determined using DC Protein Assay (Bio-Rad, USA) according to manufacturer's instructions. In brief, a standard curve was established with bovine serum albumin (BSA, 1,590 µg/ml, Bio-Rad,USA) diluted in PBS (Sigma-Aldrich, USA), ranging from 0 to 1,590 µg/ml. The samples were diluted 1:10, 1:20 and 1:40 with PBS (Sigma-Aldrich, USA), accordingly. The assay was performed in a 96-well plate (Greiner Bio-One, Austria) and absorption was measured at OD_{750} using the SpectraMax Spectrophotometer (Molecular Devices, USA). A standard curve was calculated by plotting the absorption against the concentration. The slope of the standard curve was determined and used to calculate the protein concentrations of the samples.

2.3. Cultivation of murine bone marrow derived macrophages

2.3.1. Preparation of L929 conditioned medium

L929, a mouse fibroblast cell line was grown in Dulbecco's Modified Eagle Medium (DMEM, Sigma-Aldrich, USA) supplemented with 10 % fetal bovine serum (FBS, Sigma-Aldrich, USA), 100 µg/ml Penicillin/ Streptomycin (P/S, Sigma-Aldrich, USA) and 2 mM L-Glutamine (Thermo Scientific, USA). As soon as the desired confluence of cells was reached, cells were split 1:9 into cell culture dishes. Two days later, medium was removed and 30 ml DMEM (Sigma-Aldrich, USA) supplemented with 100 µg/ml P/S (Sigma-Aldrich, USA) and 2 mM L-Glutamine (Sigma-Aldrich, USA). After 10 days, media were collected and sterile filtered (0.2 µm, Falcon, USA) and stored at -20 °C until use.

2.3.2. Isolation and differentiation of murine bone marrow derived macrophages

Bone marrow-derived macrophages (BMDMs) were isolated from bone marrow of female C57BL/6 mice. Mice were euthanized, disinfected with 70 % Ethanol (EtOH, AustrAlco, Austria) and the skin of the legs removed. Tibia and femur were prepared and transferred into a petri dish containing PBS (Sigma-Aldrich, USA). The bones were cut near the epiphysis and the inner bone cavity rinsed using a G27 needle (B.Braun, Germany) to obtain bone marrow. The resulting suspension was centrifuged for 5 min at 500 x *g* at room temrperature, the obtained pellet was resuspended in 90 % FBS and 10 % dimethyl sulfoxide

(DMSO, Sigma-Aldrich, USA) and subsequently cooled down: First 30 min on ice, then over night at -80 °C, and finally frozen in liquid nitrogen. In order to differentiate bone marrow cells to macrophages, L929 cMedium was used. Bone marrow cells were slowly thawed and centrifuged at 500 x *g* for 5 min at room temperature, seeded in standard petri dishes (day 0) and cultivated in L929 cMedium. L929 cMedium was changed on day 3, cells were split according to the respective cell density on day 4, and 1 x 10^6 cells were seeded in 6-well cell culture plates on day 7.

2.3.3. Stimulation of murine BMDM with extracellular vesicles

BMDMs were stimulated with EVs for 24 h at 37 °C and 5 % CO_2 atmosphere, depending on EV type with 0.5 µg/ml, 2 µg/ml, 5 µg/ml, 10 µg/ml, 25 µg/ml, 50 µg/ml, 100 µg/ml to examine the pro-inflammatory potential. LPS derived from E. coli strain O55:B5 served as a positive control. Additionally, two wells were left unstimulated, one constituting the negative control and one was treated with 10 µl Triton-x 100 1 hour prior harvesting the cells, illustrating maximal lactate dehydrogenase (LDH) release. Additionally, one well with plain cell culture medium only was also treated with 10 µl Triton-x 100 1 h prior cell harvest.

In order to ensure normalized conditions, the amount of EVs isolated of the isogenic mutants, was corresponding to the phospholipid levels, normalized to the respective wild-type strain. Thus, phospholipid concentration of BC25 derivates was adjusted to 5 µg and 10 µg of BC25, and respectively, phospholipid concentration of BC1*ΔplcR* was adjusted to the 50 µg and 100 µg of BC1.

After 24 hours, the cell culture supernatants were transferred to an Eppendorf tube and centrifuged at 18,000 x *g* (Eppendorf 5430 R) for 5 min at 4 °C, the supernatant was then transferred into a new Eppendorf tube and the cell pellet was discarded.

The remaining attached macrophages were harvested by washing 3 times with ice cold PBS (Sigma-Aldrich, USA) and treated with 100 µl of lysis buffer and scraped off. Cell lysates were transferred into Eppendorf tubes and incubated for 20 min on ice. The lysate was centrifuged at 18,000 x *g* (Eppendorf 5430 R) for 5 min at 4 °C. The supernatant containing the protein extract was transferred into a new Eppendorf tube and the cell pellet was discarded. Whole protein concentration was determined using Roti Quant (Carl Roth, Germany) following manufacturer's instructions. A standard curve was established with BSA (2 mg/ml; Bio-Rad, USA) in PBS (Sigma-Aldrich, USA) ranging from 0 to 100 µg/ml. The samples were diluted 1:100 with PBS (Sigma-Aldrich, USA) and transferred into a 96-well plate (Greiner Bio-One, Austria) and absorption was measured at OD_{595}.To calculate the slope, a standard curve was assessed by plotting the absorption against the concentration. The slope was then used to determine the protein concentrations of the samples.

2.3.4. Cytotoxicity of extracellular vesicles

Cytotoxicity of EVs was determined using Cytotox96® Non-radioactive Cytotoxicity Assay (Promega, USA). Briefly, 50 µl of cell culture supernatant and 50 µl of CytotoxReagent® were added to a 96-well plate. After 30 min of light-protected incubation at room temperature, 50 µl of stop solution were added. Immediately, the plate was measured at 490 nm using SpectraMax Spectrophotometer (Molecular Devices, USA). The extent of cytotoxicity was calculated using following equation:

$$\left(\frac{\text{OD (samples) - OD (plain cell culture medium)}}{\text{OD (maximal LDH release)}}\right) \text{ x } 100$$

2.3.5. Quantification of tumour necrosis factor α levels (TNF- α)

Levels of the TNF- α were quantified by using commercially available ELISA (R&D Systems, USA). The procedure was performed, as described by the manufacturer. In brief, a standard curve, using the calibrator dilutent, was established ranging from 10.9 pg/mL to 700 pg/mL. To ensure that samples are within this range, samples with strong IL-1β protein levels were diluted 1:10 with nuclease-free water (Valiant, China). 50 µl of assay dilutent and sample were added, and the plate incubated for 2 h at room temperature. The plate was washed five times with washing buffer, provided by the manufacturer, followed by incubation for 2 h with 100 µl mouse TNF-α conjugate. Again the plate was washed five times with washing buffer, and 30 min incubated protected from light with 100 µl substrate solution. Finally, 100 µl of stop solution was added, and the plate gently mixed. Optical density was measured using SpectraMax Spectrophotometer (Molecular Devices, San Jose, USA) at 450 nm and 540 nm. To subtract background values, readings measured at 540 nm were subtracted from readings measured at 450 nm. To finally calculate the results, a standard curve was established by plotting the samples with known concentrations against the OD, creating a slope. The slope was then used to analyse TNF-α levels of samples with unknown concentrations.

2.4. Proteinbiochemical methods

2.4.1. Preparation of polyacrylamide gels

Depending on the molecular weight, the appropriate separation gel, indicated in the table 2, was prepared. A glass and aluminium oxide plate was arranged in casting frames (BioRad, Hercules, USA). In the resulting gap, the separation gel solution was poured and layered with isopropanol (Sigma-Aldrich, St. Louis, USA). After polymerization (30 min), the isopropanol layer was removed, the stacking gel solution was prepared and added on top of the

separation gel. Suitable combs were placed on top immediately, and after 30 min the gel was ready to use.

Table 2: Overview of polyacrylamide gel preparations

Molecular weight of protein of interest	20 – 40 (kDa)	100 – 120 (kDa)	Same percentage for all conditions	
Separation gel	10 %	15 %	Stacking gel	4 %
1.5M Tris-buffer pH 8.8	5 ml		**0.5M Tris-buffer pH 6.8**	2.5 ml
Glycerol (Carl Roth, Germany)	0.2 ml			-
10 % SDS (Sigma-Aldrich, USA)	0.2 ml			0.1 ml
MQ-H_2O (Merck Millipore, USA)	7.8 ml	4.4ml		6.275 ml
30 % Acrylamide (Carl Roth, Germany)	6.6 ml	10 ml		1.425 ml
Tetramethylethylenediamine (Temed, Carl Roth, Germany)	30 µl			10 µl
10 % Ammonium persulfate (APS, Carl Roth, Germany)	0.2 ml			0.1 ml

2.4.2. Sodium dodecyl sulfate polyacrylamide gel electrophoresis (SDS PAGE)

At first, EV and cell lysates were treated with 4x Laemmli buffer for 5 min at 100 °C. After centrifugation at 11,300 x *g* for 3 min, 5 µg of sample were loaded onto an appropriate SDS PAGE gel. PageRuler™ Plus Prestained Protein Ladder (Thermo Scientific, USA) was used as a marker. The electrophoresis was conducted for 150 min at 90 V in 1x Running buffer. Prior to western blotting, the gel was incubated in 1x Blotting buffer for 20 min.

2.4.3. Coomassie staining

To quantify and qualify protein band patterns, protein bands were visualized by incubation in fixing solution after SDS PAGE for at least 15 min. After fixing, the solution was discarded and Page Ruler Protein Staining Solution (Thermo Scientific, USA Scientific) was applied overnight. Finally, the staining solution was removed and the gel was destained until bands were visible.

2.4.4. Western blotting

Western blotting was performed with EV lysates and BMDM cell lysates. For semi-dry blotting, whatman paper (GE Healthcare Life Sciences, UK) and nitrocellulose membrane (GE Healthcare Life Sciences, UK) were incubated for at least 20 min in 1x Blotting buffer. Prior to incubation, nitrocellulose membrane was activated for 60 seconds in USA-H_2O

(Merck Millipore, USA). For blotting, Transblot SD Semi Dry Transfer Cell (BioRad, USA) was used. The layers were assembled as following, from bottom to top: two pieces of whatman paper, one piece of nitrocellulose membrane, one piece of polyacrylamide gel and two pieces of whatman paper. Duration and voltage of semi-dry blotting was applied depending on molecular weight. Proteins with a molecular weight of 20-40 kDa were blotted at 15 V for 20 min, 40 kDa - 50 kDa proteins were blotted at 15 V for 18 min followed by 18 V for 12 min, and 50 kDa - 120 kDa proteins were blotted at 15 V for 40 min.

For western blots of EV lysate, the membrane was stained with Ponceau S (PanReac, USA) after blotting in order to visualize the total protein amount. Blocking of the membrane was performed for 1 h with 10 ml 5 % milk powder in TBS-T followed by three washing steps for 5 min with TBS-T. Primary antibodies were diluted according to table 3, in 10 ml 1 % milk powder in TBS-T and incubated overnight at 4 °C with shaking. Before and after application of the secondary antibody, the membrane was washed three times for 5 min with TBS-T. Secondary antibodies were diluted according to table 3 in 10 ml 1 % milk powder in TBS-T and incubated for 1 h at room temperature, with shaking

For western blots of BMDM cell lysate the reaction was directly blocked after blotting. Blocking of the membrane was performed for 1 h with 10 ml 5 % milk powder in pyTBS-T, followed by three washes for 5 min with pyTBS-T. Proteins bands were detected using commercially available antibodies (see table 3 below). Primary antibodies were diluted in 10 ml 1 % milk powder in pyTBS-T and incubated over night at 4 °C with shaking. Before and after application of the secondary antibody, the membrane was washed three times for 5 min with pyTBS-T. Secondary antibodies were diluted in 10 ml 1 % milk powder in pyTBS-T and incubated for 1 h at room temperature. To determine the total protein amount, the membrane was stripped for 5 min using stripping buffer, blocked for 30 min with 10 ml 5 % milk powder and incubated again with the primary antibody against the house-keeping protein panErk.

For detection of proteins, Super Signal West Pico Chemiluminescent Substrate (Thermo Scientific, Waltham, USA) was used according to manufacturers' protocol and chemiluminescence was detected.

Table 3: Antibodies used for western blotting

Primary antibody		Secondary antibody (horse radish peroxidase conjuageted	
Specificity & Source	Working Dilution	Specificity & Source	Working Dilution
Antibodies used for EV western blots			
Anti-NheB (provided by Richard Dietrich)	1:40	anti-Mouse (Jackson Immuno Research, USA)	1:20,000
Anti-Smase (provided by Richard Dietrich)	1:40	anti-Mouse (Jackson Immuno Research, USA)	1:20,000
Anti-Flagellin (provided by Nadja Jeßberger)	1:1000	anti-Rabbit (Jackson Immuno Research, USA)	1:1000
Anti-phospholipase C (antikörper-online.de)	1:40	anti-Rabbit (Jackson Immuno Research, USA)	1:1000
Antibody used for cell lysate western blots			
Anti-IL-1β (R&D Systems, USA)	1:1000	anti-Goat (Santa Cruz, USA)	1:10000
Anti-panERK (BD Biosciences, USA)	1:4000	anti-Mouse (Jackson Immuno Research, Bar Harbor, USA)	1:20000

2.5. Characterisation of EVs

2.5.1. Determination of phospholipid levels

To quantitate the amount of phospholipids the Phospholipid Assay Kit (Sigma-Aldrich, USA) was used, according to manufacturer's protocol. In brief, samples were diluted to a final volume of 40 µl with PBS (Sigma-Aldrich, USA) and fluorescence was detected using a standard curve. The standard curve was established using 2 mM phosphatidylcholine provided by the kit and covered a range from 0 µM to 20 µM. Flourescence was detected at

$OD_{excitation}$ 530 nm and $OD_{emmission}$ 585 nm using SpectraMax Spectrophotometer (Molecular Devices, USA). To calculate the phospholipid concentrations of the samples, the slope of the standard curve was assessed, and applied to calculate the phospholipid concentrations of the samples

2.5.1. Quantitation of sphingomyelinase activity

Amplex® Red Sphingomyelinase Assay Kit (Promega, USA) was used to measure sphingomyelinase (SMase) activity. 10 µg the EV fraction were used and assayed, following the manufacturers protocol. To determine enzymatic activity, samples were compared to a sample with known concentration, provided by the manufacturer. Reactions were incubated protected from light for 40 min at 37 °C. Fluorescence was measured at $OD_{excitation}$ = 530 nm and $OD_{emission}$ = 585 nm, using SpectraMax Spectrophotometer (Molecular Devices, USA).

2.5.2. Transmission electron microscopy

To obtain ultra-thin sections, 70 µg of the EV fraction was pelleted by ultra-centrifugation at 125,000 x *g* for 1 h at 4 °C. The supernatant was cautiously removed and the pellet was fixed in 3 % buffered glutaraldehyde (pH 7.4, Merck, Germany) for 48 h. Prior to postfixation in 1 % osmium tetroxide (Electron Microscopy Sciences, USA) for 2 h at room temperature, the pellet was preemedded in 1.5 % Agar and washed three times in 0.1 M phosphate buffer (Soerensen pH 7.4). Embedding was performed via epoxy resin (Serva, Germany), ethanol series and propylene oxide (Sigma-Aldrich, USA). For pre-evaluation, sections were cut at 0.8 µm and contrasted with toluidine blue (Carl Roth, Germany). Ultrathin sections were cut at 70 nm and stained with alkaline-lead citrate (Merck, Germany) and methanolic-uranyl acetate (Fluka Chemie, AG, Switzerland). Each sample was evaluated for the presence of EVs in a in a transmission electron microscope (Zeiss EM 900) equipped with a digital Frame-Transfer-CCD- camera (Tröndle TRS, Germany).

2.5.3. TEM image analysis

The samples were visualized on a transmission electron microscope and screened for EV structures. Diameters of EVs were assessed by Image J (Schneider *et al*., 2012) and multiplied by the magnification factor, according to the table below.

Table 4: Magnification factors

Magnification	Magnification factor
20,000	227.2727273
30,000	156.25
50,000	100
85,000	60.97560976

2.5.4. Exactive Orbitrap LC-MS/MS

Prior to proteomic analyses, EVs were precipitated using trichloroacetic acid (TCA) (Carl Roth, Germany). 70 µg of the EV fraction was diluted with 1 ml of MQ-H_2O (Merck Millipore, USA) and 100 µl ice-cold TCA was added. The solution was incubated overnight at 4 °C and subsequently centrifuged for 20 min at 20,000 x *g* at 4 °C (Hettich Centrifuge 5430R, Eppendorf, Germany). The supernatant was discarded, and the remaining protein pellet was washed with 1 ml ice-cold acetone (Carl Roth, Germany) for three times (20 min, 20,000 x *g,* 4 °C. After the last centrifugation step, the remaining protein pellet was resuspended in 35 µl buffer containing 6 M urea (Carl Roth, Germany), 2 M thiourea (Carl Roth, Germany) and 10 mM Tris (Carl Roth, Germany). The final protein concentration was determined using SDS PAGE and Coomassie Staining. As a reference, a protein ladder and a sample with known concentration were used.

30 µg of the protein were filled up to 500 µl with 8 M urea in 50 mM Tris and were loaded onto an Amicon 10kDa filter. The solution was centrifuged two times for 20 min at 10,000 x g. The proteins were reduced with 200 mM DTT (Sigma-Aldrich, USA) at 37 °C for 30 min and alkylated with 500 mM iodacetamid (Sigma-Aldrich, USA) at 37 °C for 30 min. After two washes with 100 µl 50 mM Tris, digestion was carried out using Trypsin/LysC Mix (Promega, USA) in a ratio of 1:25 (Protease:Protein) over night. Digested peptides were recovered by washing three times with 50 µl of 50 mM Tris (Carl Roth, Germany) and acidified with 1µl concentrated trifluoroacetic acid (TFA) (Fisher Scientific, USA). Prior to LC-MS/MS analysis, peptide extracts were desalted and cleaned up, using C18 spin columns (Pierce, USA). The dried peptides were re-dissolved in 300 µl 0.1% TFA, of which 3 µl were injected into the LC-MS/MS system. Peptides were separated on a nano-HPLC Ultimate 3000 RSLC system (Dionex, USA). Sample pre-concentration and desalting was accomplished with a 5 mm Acclaim PepMap µ-Precolumn (300 µm inner diameter, 5 µm particle size, and 100 Å size; Dionex, USA). For sample loading and desalting, 2 % acetonitrile (ACN), (Merck, USA) in ultra-pure H_2O with 0.05 % TFA (Fisher Scientific, USA) was used as a mobile phase with a flow rate of 5 µl/min.

Separation of peptides was performed on a 25 cm Acclaim PepMap C18 column (75 µm inner diameter, 3 µm particle size, and 100 Å pore size, Dionex, USA) with a flow rate of 300 nl/min. For mass spectrometric analysis, the LC was directly coupled to a high resolution Q Exactive HF Orbitrap mass spectrometer.

MS full scans were performed in the ultra-highfield Orbitrap mass analyzer in ranges m/z 350−2000 with a resolution of 60,000. The maximum injection time (MIT) was 50 ms and the automatic gain control (AGC) was set to $3e^6$. The top 10 intense ions were subjected to

Orbitrap for further fragmentation via high energy collision dissociation (HCD) activation over a mass range between m/z 200 and 2000, at a resolution of 15 000 with the intensity threshold at $4e^3$. Ions with charge state +1, +7, +8 and >+8 were excluded. Normalized collision energy (NCE) was set at 28. For each scan, the AGC was set at $5e^4$ and the MIT was 50 ms. Dynamic exclusion of precursor ion masses over a time window of 30 s was used to suppress repeated peak fragmentation.

For EVs derived of BC25 and BC25*ΔnheBC*, two biological replicates were measured, for all other strains only one biological sample was available. Proteins appearing in all two biological replicates of BC25 and BC25*ΔnheB*C were considered for further analyses

2.5.5. Statistical analysis

Data were analysed using GraphPad Prism version 8.0 for Max OS X (GraphPad Software Inc., USA). Statistical significance of differences between EV treatments was tested using one-way ANOVA with Dunnett's multiple comparison test. To examine normal distributions of EVs, Anderson-Darling test was used. Significance between EV sizes was calculated by an unpaired t-test. Differences were considered significant at p values of $p < 0.05$.

3. Results

3.1. Characterization of extracellular vesicle-like structure

3.1.1. Establishment of vesicle isolation method and toxin detection

Unpublished data indicates that *Bacillus cereus* secretes EVs. A protocol, using centrifugal and size-exclusion mechanisms, was therefore established to purify EVs. Prior to filtration of the bacterial culture (0.2 µm) the bacterial culture was centrifuged twice to remove bacterial cells and cell debris. Subsequently, the clear filtrate was applied on size-exclusion filtration units (100 kDa cut-off). The supernatant was obtained and subjected to ultra-centrifugation to gain a pellet consisting of EVs. However, by immunoblotting, a protein <100 kDa NheB was detected in this fraction, suggesting its association with larger structures. In addition, the presence of flagellin (50 kDa) was also demonstrated in both, the EV fraction and the flow-through by immunoblotting. Further virulence factors (Collagenase A and PI-phospholipase C) were only present in the flow-through (Fig. 8).

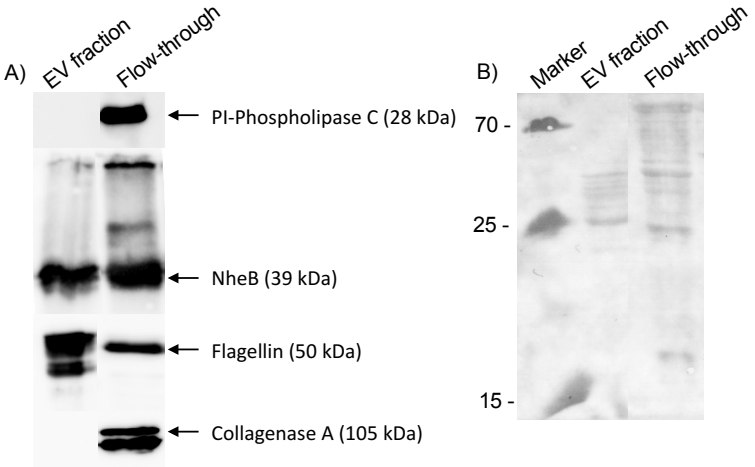

Figure 8: Detection of virulence factors in the EV fraction and the flow-through of BC25.
Western blot using PI-Phospholipase C, NheB, Flagellin and Collagenase A antibodies and HRP-conjugated secondary antibodies to detect virulence factors in the EV fraction and the flow-through **(A).** For loading control, the membrane was stained prior to antibody incubation with Ponceau S **(B).**

3.1.2. Influence of environmental conditions on protein concentration in *B. cereus* EVs

In order to evaluate if different culture media influence the protein amount in the EV fraction, BC25 was cultured under laboratory conditions (LB, 30 °C, shaking) as well as host mimicking conditions (cRPMI, 37 °C, 7 % CO_2, static) and harvested after 2 h, 6 h and 17 h inoculation.

Under laboratory conditions, no protein was detected in the EV fraction after 2 h inoculation, whereas 59.0 µg were detected after 6 h inoculation and 106.8 µg were detected after 17 h inoculation (Fig. 9A). Contrary, under host-mimicking conditions, 13.73 µg protein was

yielded in the EV fraction after 2 h inoculation, 37.16 µg protein after 6 h inoculation and 33.0 µg protein after 17 h inoculation (Fig. 9B).

Bacteria, cultivated in LB for 2 h, grew to OD_{600}= 0.39, contrary to bacteria cultured in cRPMI, which reached an OD_{600}= of 0.79. After 6 hours of growth, bacteria cultured in LB reached an OD_{600}= 3.85 whereas bacteria grown in cRPMI reached an OD_{600}= of 2.30. Bacteria cultured for 17 hours in LB grew to OD_{600}= 6.62, however, growth of bacteria cultured in cRPMI stagnated and grew to OD_{600}= 2.25 (Fig. 9). Thus, host mimicking condition triggered earlier protein secretion, but also resulted in stagnation after longer incubation.

As shown in figure 9, vesicle proteins were not detectable after cultivation of 2 h in LB media (Fig. 9A), but in cRPMI (Fig. 9B). However due to stagnation of bacterial growth in cRPMI, the highest amount of EV could be yielded using LB with a culture time of 17 h at 30 °C shaking. In addition, to compare protein band patterns, the EV fraction was also subjected to SDS Page (Fig. 9C).

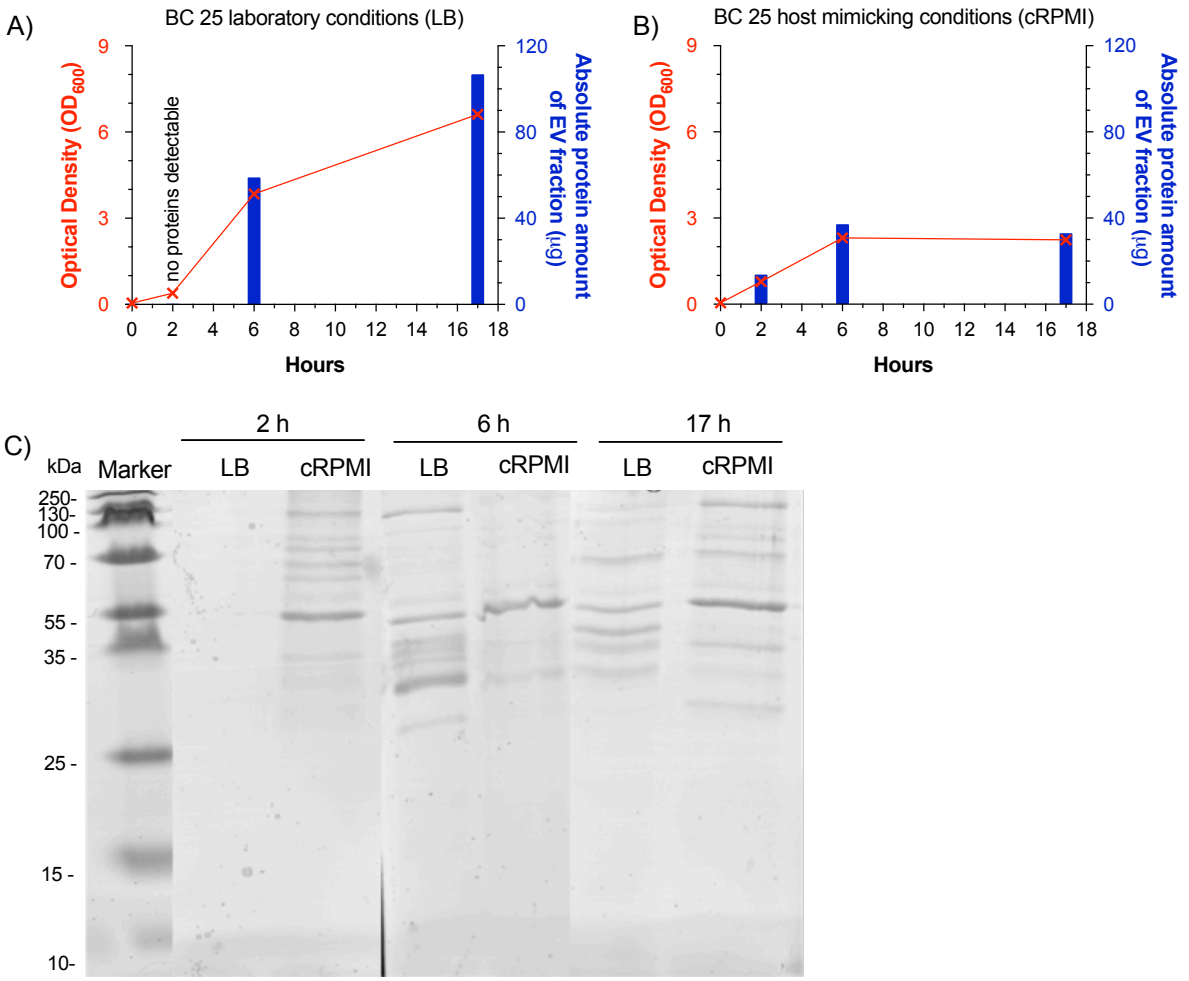

Figure 9: Influence of culture conditions on bacterial growth and EV production of B. cereus BC25. Comparison of bacterial growth (OD, red line) and proteins in the EV fraction (blue bars) cultivated in LB (A) and cRPMI (B). Protein band patterns of each conditions were compared by SDS PAGE. As no protein was detectable after 2 h in LB, maximal applicable volume (25 µl) of the EV fraction were loaded, for all other conditions a standardized amount (5 µg) were used (C).

3.1.3. Characterisation of EVs produced by *B. cereus* mutant strains

To assess how the bacterial genetic background effects the EV production of B. cereus, a set of isogenic mutants of BC25 (BC25*ΔnheBCΔsph,* BC25*Δsph*, BC25*ΔnheBC),*the enteropathogenic reference strain ATCC 14579 (further referred to as BC1) and its derivative BC1*ΔplcR* were used for EV production. Secretion of EVs, containing proteins was verified for all strains by SDS PAGE (Fig. 10A). However, the pattern of BC1*ΔplcR* differed, compared to its parent strain, whereas those of the BC25 derivatives resembled that of the wild type (Fig. 10A).

To further examine the toxigenic potential of EVs, the presence of NheB and SMase was tested. Ponceau S staining, performed prior to antibody incubation, confirmed that an equal protein amount was applied for each lane (Fig. 10B). According to the biological background of the strain set, BC25 showed expression of both toxins, whereas BC25*ΔnheBCΔsph* showed no expression of these proteins (Fig. 10C). A signal for SMase could by detected in BC25*ΔnheBC,* whereas a signal for NheB could be observed in BC25*Δsph* (Fig. 10C). Signals for both toxins could also be identified in BC1, although weaker. BC1ΔplcR showed only marginal NheB expression (Fig. 10C).

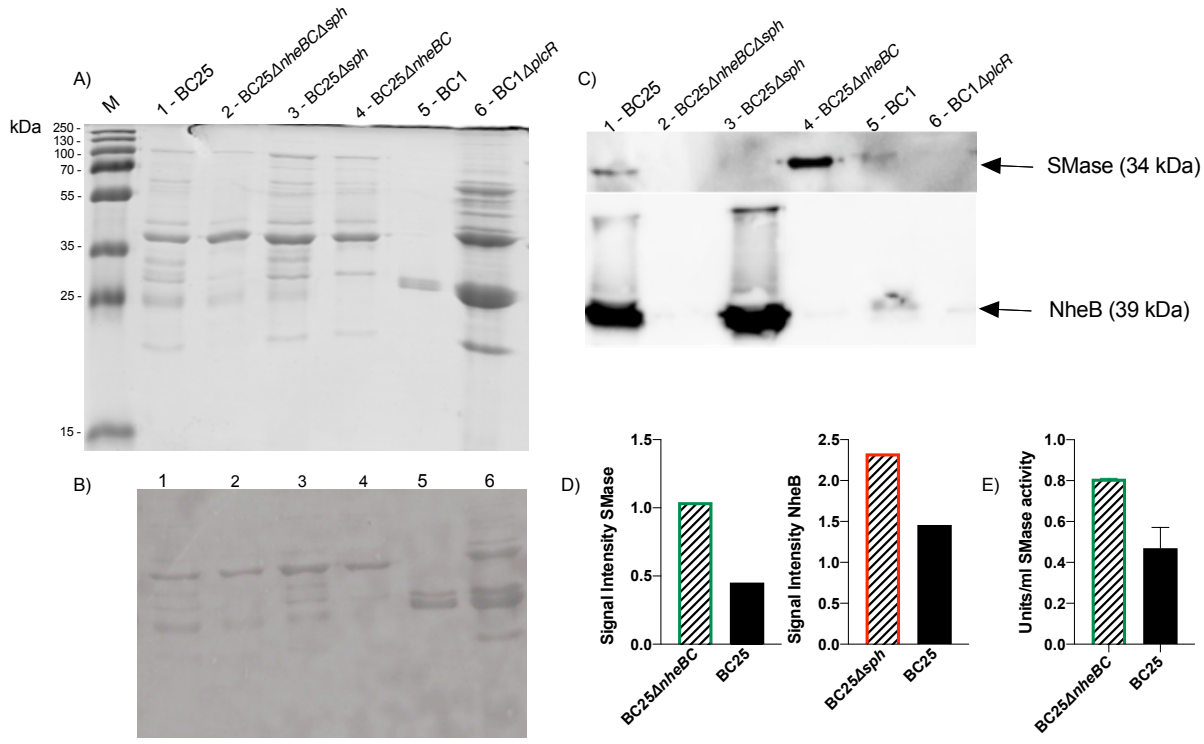

Figure 10: Protein pattern and toxin detection of mutant strain set. Coomassie stained SDS PAGE visualizes protein band patterns of EV fractions in **(A)**. A representative Ponceau S staining of the membrane is shown in **(B)**, samples were applied in the same order as in panel **(a)** on the gel. Western blot analysis shows the expression **(C)** of SMase and NheB. Panel **(D)** shows signal intensities of total protein amount normalized to western blot signal intensities of the parent strain BC25 compared to BC25*ΔnheBC and* BC25*Δsph,* respectively. Panel **(E)** compares SMase activity in the parent strain BC25 to the activity in BC25*ΔnheBC.* Error bars represent arithmetic means and standard deviation from two technical replicates.

In addition, toxigenic potential of EVs was examined by quantification of SMase activity. In accordance to the results by immuno blotting, enhanced SMase activity was measured in BC25*Δnhe*BC (0.89 units/ml) compared to its parent strain, BC25 (0.47 units/ml). (Fig. 10E).

3.1.4. Proteomic analysis of EVs from *B. cereus* strains and isogenic mutants

Purified EVs were analysed by Exactive Orbitrap LC-MS/MS, in order to identify proteins enclosed in these bacterial extracellular structures. 405 and 301 proteins were identified for each sample of BC25, respectively. For BC25*ΔnheBC* EVs, 372 and 330 proteins were identified, respectively. For further annotation of proteins, only proteins present in both replicates were considered (data not shown) and are indicated by the suffix '_same'. 363 proteins were identified in BC25*Δsph* EVs, 129 proteins in BC25*ΔnheBCΔsph* EVs, 212 proteins in BC1 EVs, and 410 proteins in BC1*ΔplcR* EVs.

Among the identified proteins, 46 were found in the BC25 parental strain and the isogenic mutants (Fig. 11A), further referred to as core proteins. 21 proteins were found exclusively in the parent strain, and 6 unique proteins were identified in the EVs of all BC25 mutants. In BC1, 212 proteins were identified and in BC1*ΔplcR,* 410 proteins were identified, resulting in a to a total of 158 proteins commonly identified in both strains (Fig. 11B).

The core protein set of BC25 EV comprised proteins associated with flagellar motility (21.28 %), pathogenesis (6.38 %), transmembrane transporters (4.26 %), metabolism (34.04 %), phage-associated proteins (10.64 %) and so far uncharacterized proteins (14.39 %) (Fig. 11C). Similar distributions are found in BC1 and its isogenic mutant: flagellar motility (10.0 %), pathogenesis (0 %), transmembrane transporters (8.97 %), metabolism (46.79 %), phage-associated proteins (5.13 %) and so far uncharacterized proteins (6.14 %). However, no proteins belonging to the GO categorie "pathogenesis-associated proteins" were found.

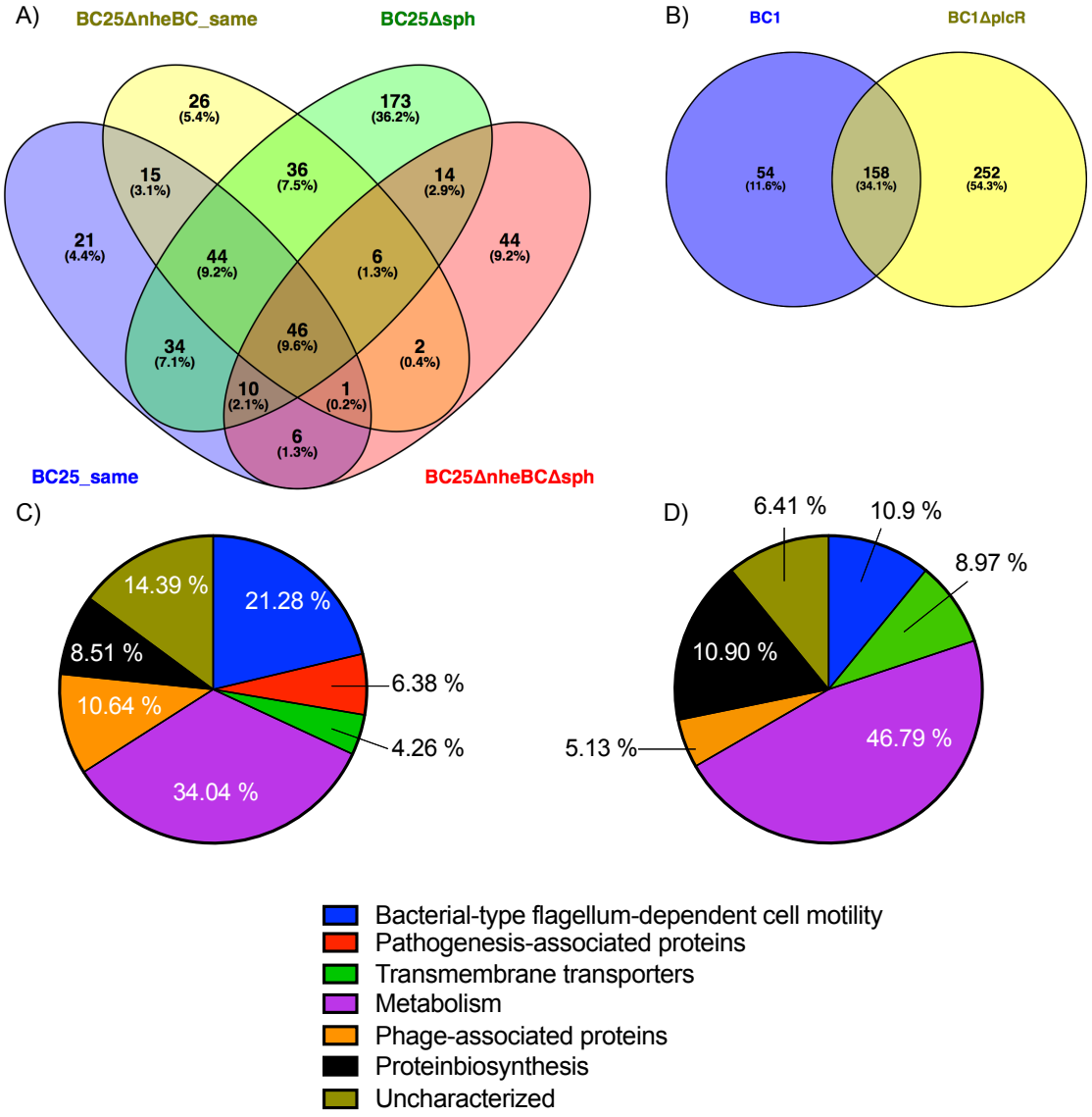

Figure 11: Venn diagrams showing the protein overlap between the respective strains and the putative function for identified proteins. Proteins were mapped with respect to the BC25 and isogenic mutants **(A)** or the BC1 and isogenic **(B)**. The results of the GO term annotation of the core proteins found in BC25 and BC1 with regard to the isogenic mutants are depicted in **(C)** and **(D)**, respectively.

3.1.5. Phospholipid content of EVs

The presence of phospholipids could be demonstrated for each EV isolate. In general, a varying amount of phospholipids was found for each EV isolate. The EV fraction of BC25*Δsph* showed the highest amount of phospholipids (25.18 µM), followed by the BC25 EV fraction (12.26 µM). Phospholipid concentrations measured in the BC25*ΔnheBC* EV fraction (10.31 µM) were similar to the amount of BC25, whereas the EV fraction of BC25*ΔnheBCΔsph* (2.41 µM) and BC1*ΔplcR* (1.55 µM) showed a rather low amount of phospholipids. For BC1, phospholipid levels could not be quantified, presumable due to the low amount of phospholipid (Fig. 12A).

For further experiments, it was necessary to adjust the phospholipid levels of the isogenic mutants to the parent strains, therefore, the phospholipid content was, measured again, after normalization (Fig. 12B). Furthermore, phospholipid content for BC1 EVs was adjusted to 14 µg. After normalisation, phospholipid levels for BC25 (10.46 µM), BC25*ΔnheBCΔsph* (7.439 µM), BC25*Δsph* (13.67 µM), BC25*ΔnheBC* (10.18 µM) BC1 (1.02 µM), BC1*ΔplcR* (0.48 µM), could be adjusted to the respective parent strain. In summary, the presence of phospholipids indicates the assumed amount of secreted membrane derived structures – such as extracellular vesicles.

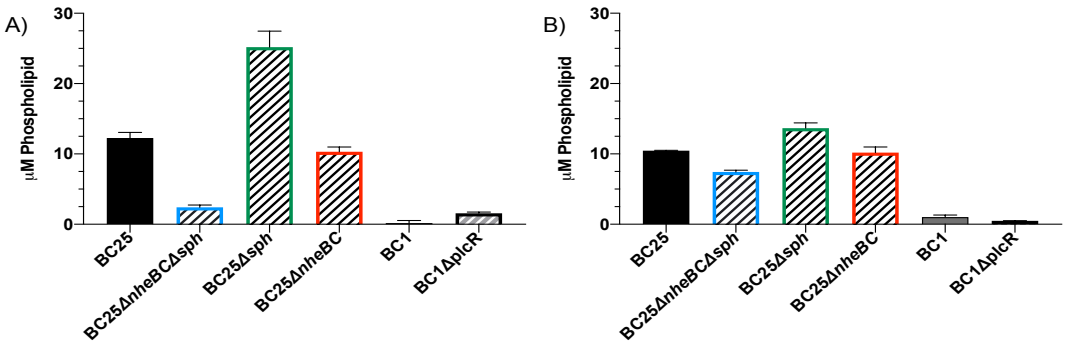

Figure 12: Phospholipid concentration of each EV fraction isolate. In panel (**A),** 10 µg of the EV fraction were assayed. Panel (**B)** depicts the phospholipid amounts after normalisation to BC25 and BC1. Two independent measurements were performed, using duplicates. Error bars represent arithmetic means and standard deviation.

3.2. Visualization of EVs by transmission electron microscopy

In order to visualize EV structures, transmission electron microscopy was carried out (TEM) using the fraction from bacterial cultures (grown in LB, 17 h, 30 °C) containing the isolated EVs. The imaging revealed a vast variety of circular structures, representing the EVs, bordered by an evenly thick membrane (see Fig. 13). These structures can be easily detected as they displace the fibrous background, presumably representing flagella of *B. cereus* (indicated by blue arrow). A representative wide-field picture (Fig. 13A) shows that several structurally diverse EVs are grouped together (indicated by red arrows).

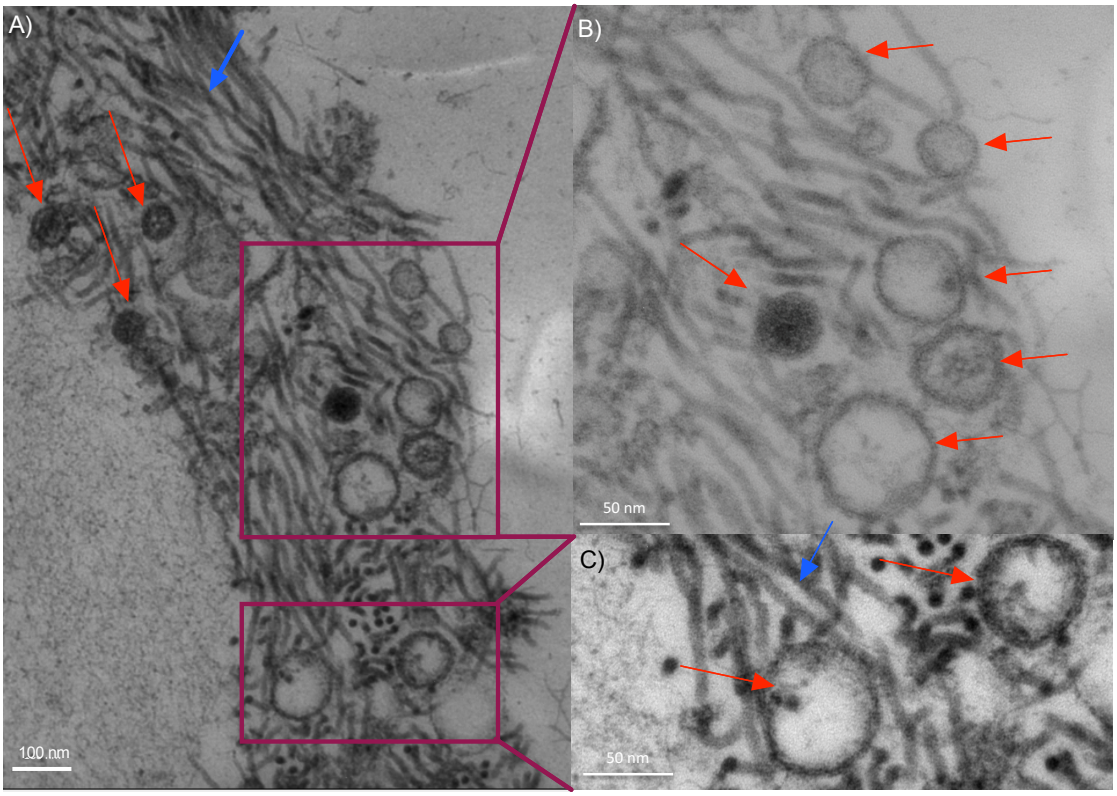

Fig. 13: TEM image of EVs purified from BC25. Red arrows indicate EVs, whereas blue arrows indicate fibrous background. Image **(A)** shows a representative wide-field view, whereas **(B)**and **(C)** enlarges the section marked with the purple frame.

To further classify their vast variety, four categories regarding their sizes, shapes and shades EVs were grouped into: ‘dark’, ‘bright’, ‘nested’ and ‘other’. Dark EVs represent electron-dense EVs, the surrounding membrane is not distinguishable from the inner EV content. Bright EVs depict structures, of which the membrane is clearly visible. Nested EVs represent structures with other EVs enclosed. Structures classified as other are strain-specific EV structures that cannot be assigned to any other EV structure.

EVs secreted by BC25 (Fig. 14, first row) occurred mainly as bright EVs. However, dark EVs and nested EVs were also present. EVs purified of BC25*ΔnheBCΔsph* (Fig. 14, second row), were mostly covered by a cloudy dark coat (Fig. 14) and only one dark EV was detected. Nonetheless, other EV structures of BC25*ΔnheBCΔsph* resembled those in BC25 (Fig. 14). EVs purified of BC1*ΔplcR* also comprised a vast structural diversity; Bright, dark as well as nested EVs were present (Fig. 14, sixth row). Contrary to BC25, BC25*ΔnheBCΔsph* and BC1*ΔplcR*, no dark EVs were discovered in BC25*Δsph,* BC25*ΔnheBC* and BC1. Nested EVs were present in each isolate, except BC1. Nested EV structures were identified to enclose up to three other EVs (Fig. 16). Enclosed EVs could structurally resemble either bright or dark EVs (Fig. 14, third column).

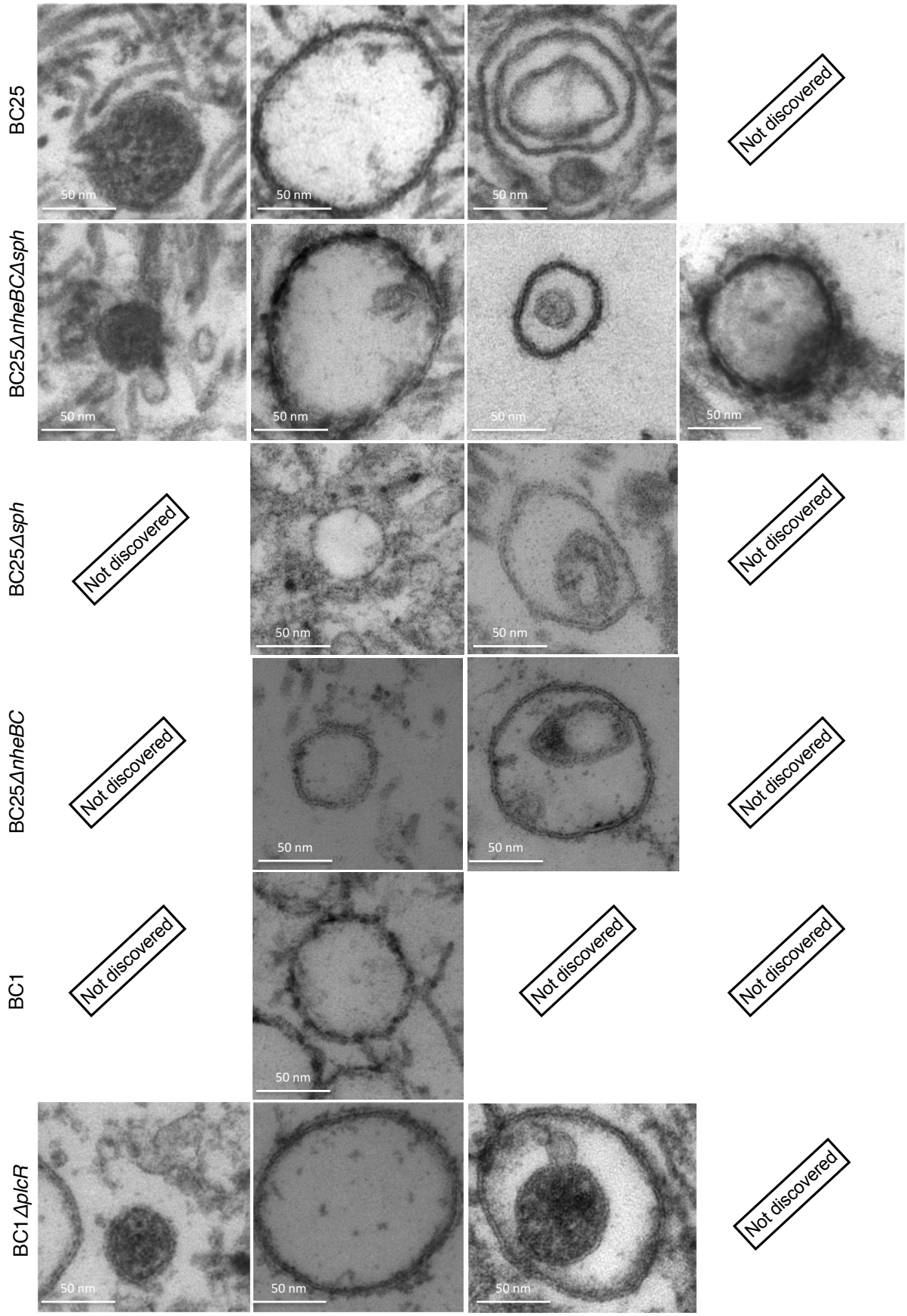

Fig. 14: TEM images of EVs obtained from BC25, BC1 and the isogenic mutants. Ultra-thin slices (70 nm) were used for imaging of EV stuctures. The first column represents dark, the second bright, the third nested and the last uncharacterized EV forms.

Fig. 15 depicts the measured sizes of EVs, which are –according to the EV structure – heterogeneous. Since the EV diameters were not normally distributed, the median was calculated. Based on the median EV size, EVs isolated of BC1 were of largest (125 nm), followed by BC25*Δsph* EVs (77.36 nm), BC25 (71.31 nm), BC1*ΔplcR* EVs (64 nm), BC25*ΔnheBCΔsph* (55.46 nm) and BC25*ΔnheBC* (47.98 nm).

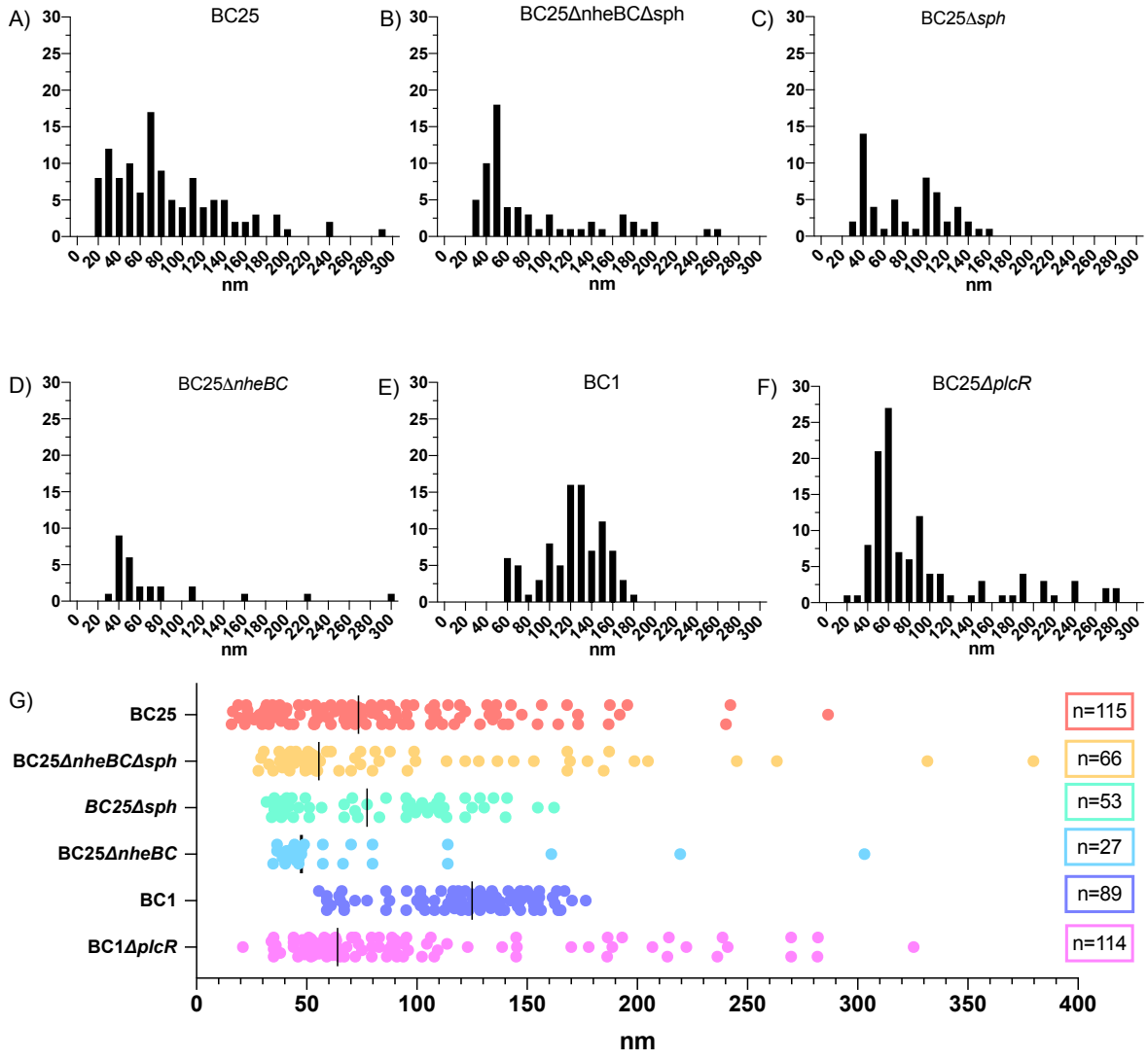

Fig. 15: EV sizes of the strain-set illustrated by histograms and scatter plots. For each strain (A – F), diameter sizes of EVs were determined, frequency distribution was calculated and plotted according to their frequencies. The median was calculated and is depicted by a line in panel (G). The number of EVs measured is listed on the right side of the scatter plot.

To further characterize EV sizes, diameters of dark EVs were compared to diameters of bright EVs. Only dark EVs and bright EVs discovered in BC25 and BC1*ΔplcR,* were used for analysis. Diameters of bright EVs do not correspond to a normal distribution (Fig. 16A), whereas diameters of dark EVs did (Fig. 16B). The mean sizes were calculated, revealing significant differences between dark and bright EVs within each strain (Fig. 16C). However, no significant difference in the EV diameters between the strains was detected. In total, EV sizes range from 20 to >300 nm.

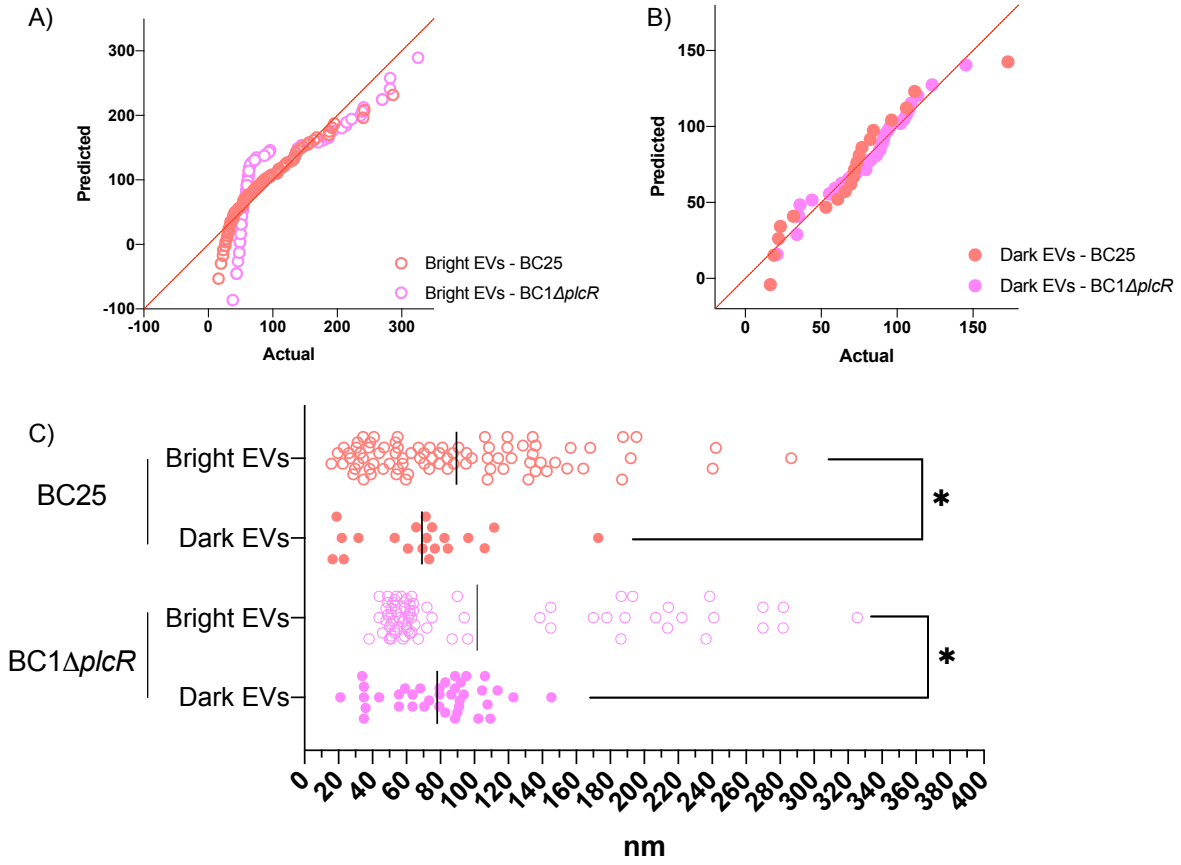

Fig. 16: Comparison of dark and EV sizes. Panel **(A)** and panel **(B)** depict QQ-blots of bright and dark EVs, panel **(A)** shows a skewed distribution of diameters of bright EVs, whereas **(B)** demonstrates a normal distribution of dark EVs. Panel **(C)** compares diameter sizes of dark and bright EVs from BC25 and BC1*ΔplcR.* To test significance of normal distributions, Anderson-Darling test was used. Differences between dark and bright EV sizes were calculated by an unpaired t-test.

3.3. Pathogenic potential of EVs

In order to evaluate the pathogenic potential of EVs, a bone marrow-derived macrophage (BMDM) culture was established, and the cytotoxic and immuno-stimulatory potential was examined by measuring proinflammatory markers, such as pro-IL1β and TNF-α. During preliminary experiments, it was observed that application of 100µg/ml by BC25 EVs, but not by BC1 EVS, led to full cell lysis.

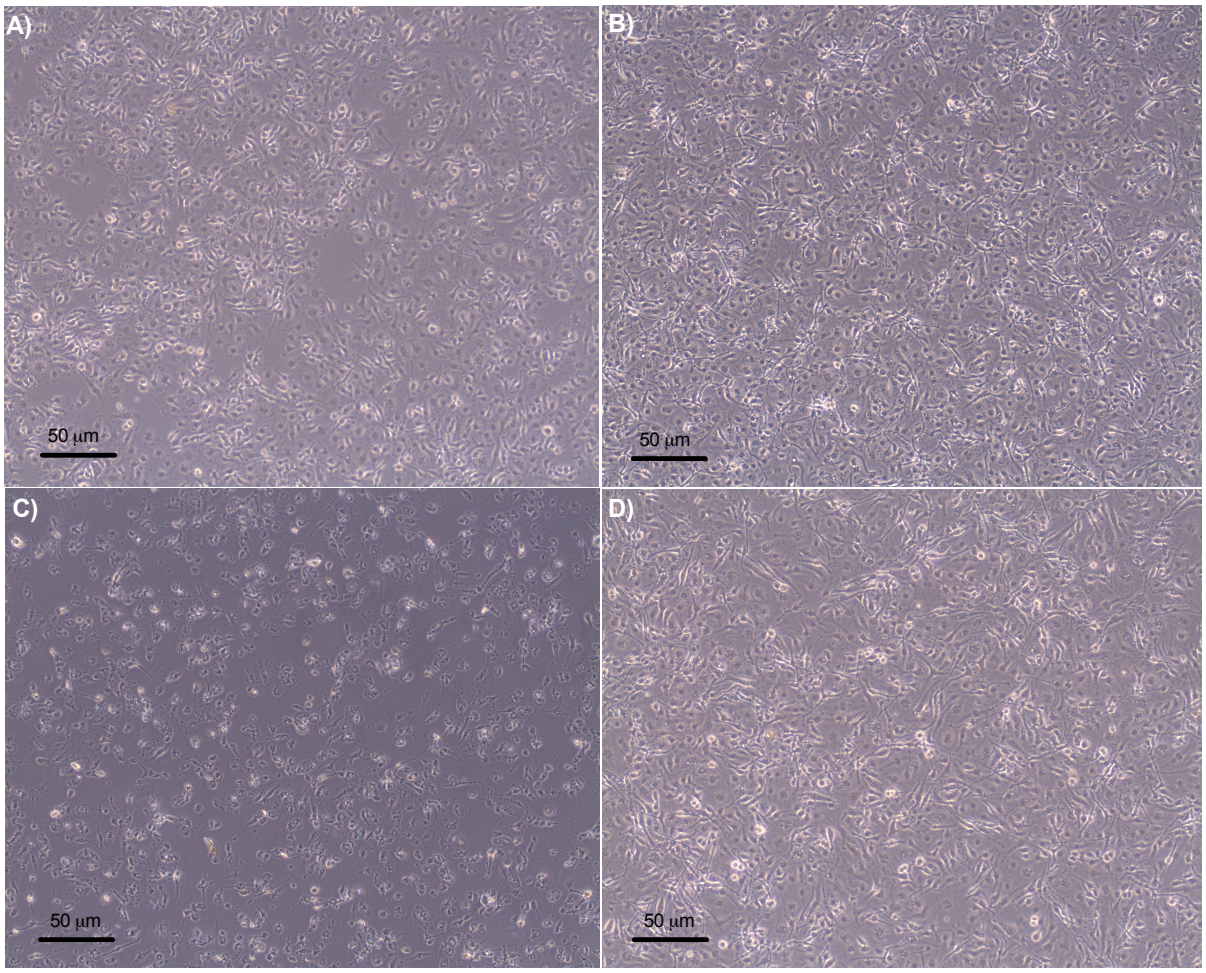

Fig. 17: Impact of EVs on BMDM culture. After 6 h stimulation with **(A)** no EVs, **(B)** 100 ng/ml LPS, **(C)** 100 µg/ml BC25 EVs and **(D)** 100 µg/ml µg BC1 EVs massive cell lysis was detectable in BMDMs stimulated with EVs purified from BC25.

Different concentrations of BC1 and BC25 EVs were applied on BMDMs, to test if cells respond to *B. cereus* EVs in a dose-dependent manner. LDH release was measured to determine the cytotoxic effects (Fig. 18A), whereas pro-IL-1β and TNF-α expression was measured to assess immunostimulatory effects (Fig. 18 B-E).

Co-incubation of BMDMs with 5 µg/ml, 10 µg/ml, 15 µg/ml, 25 µg/ml, 50 µg/ml BC25 EVs, and 100 ng/ml LPS, resulted in 45.3 %, 69.7 %, 81.3 %, 89.3 %, 89.18 % and 21.5 % cytotoxicity, respectively. This was significantly higher than the amount of LDH released from unstimulated cells. No significant effects were observed in cells stimulated with 0.5

µg/ml (3.415 % Cytotoxicity) and 2 µg/ml (7.674 % Cytotoxicity) compared to unstimulated cells (Fig. 18A).

EVs isolated from BC1 showed lower cytotoxic potential, significant differences were detected upon stimulation with 100 µg/ml BC1 EVs (16.89 % Cytotoxicity) and 100 ng/ml LPS (21.55 % Cytotoxicity) compared to unstimulated cells. No significant effects were detected in cells incubated with 0.5 µg/ml (4.26 % cytotoxicity), 2 µg/ml (3.98 % cytotoxicity), 10 µg/ml (5.55 % cytotoxicity) and 50 µg/ml (10.70 % Cytotoxicity) BC1 EVs (Fig. 18A).

Expression of pro-IL-1β was significantly stimulated by 15 µg/ml, 25 µg/ml and 50 µg/ml EVs purified of BC25. However, weak signals were also measured by stimulation with 5 and 10 µg/ml BC25 EVs. In contrast, EVs isolated of BC1 could not significantly stimulate pro-IL-1β expression, however, expression of pro-IL-1β could be detected in cells stimulated with 2, 10, 50 and 100 µg/ml BC1 EVs at low levels, which are comparable to application of 100 ng/ml LPS (Fig. 18B-C).

In addition to pro-IL-1β, TNF-α expression was also stimulated by EVs. Significant differences in TNF-α expression were only detected towards LPS (5.76 ng/ml). Cells stimulated with BC25-derived EVs caused a stronger TNF-α response than with BC1-derived EVs. Expression levels of TNF-α were as following: Cells stimulated with 0.5 µg/ml BC25 EVs expressed 0.65 ng/ml, with 2 µg/ml 0.33 ng/ml, with 5 µg/ml 3.32 ng/ml, with 10 µg/ml 1.33 ng/ml, with 15 µg/ml 4.59 ng/ml, with 25 µg/ml 3.48 ng/ml, and with 50 µg/ml 4.02 ng/ml TNF-α. Stimulation with 0.5 µg/ml EVs of BC1 resulted in 0.29 ng/ml, with 2 µg/ml in 0.26 ng/ml, with 10 µg/ml in 0.47 ng/ml, with 50 µg/ml in 0.44 ng/ml and with 100 µg/ml in 0.12 ng/ml TNF-α (Fig. 18E).

A)

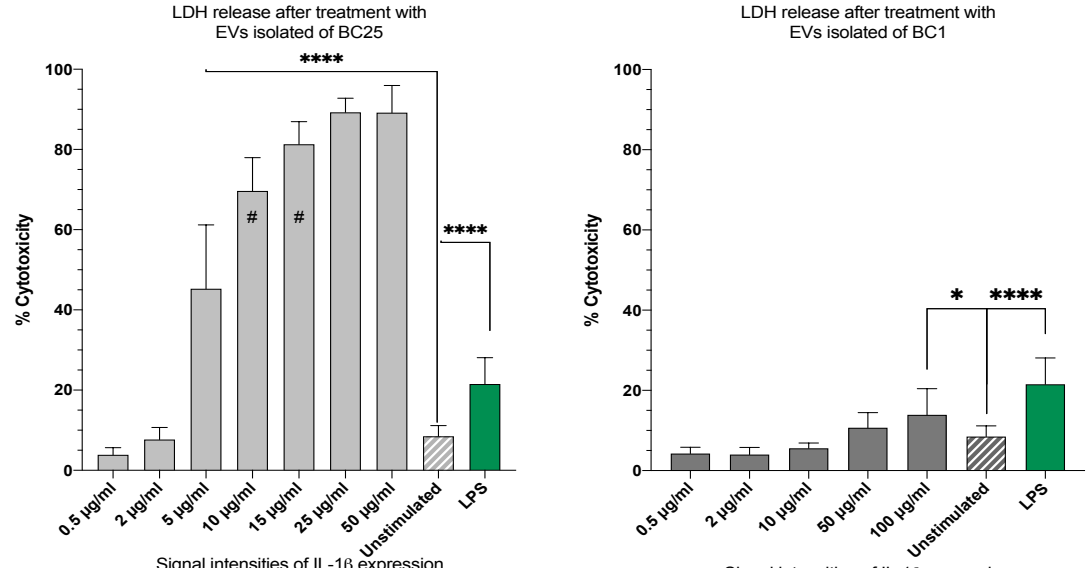
LDH release after treatment with EVs isolated of BC25
% Cytotoxicity
0.5 µg/ml
2 µg/ml
5 µg/ml
10 µg/ml
15 µg/ml
25 µg/ml
50 µg/ml
Unstimulated
LPS
LDH release after treatment with EVs isolated of BC1
100 µg/ml

B)

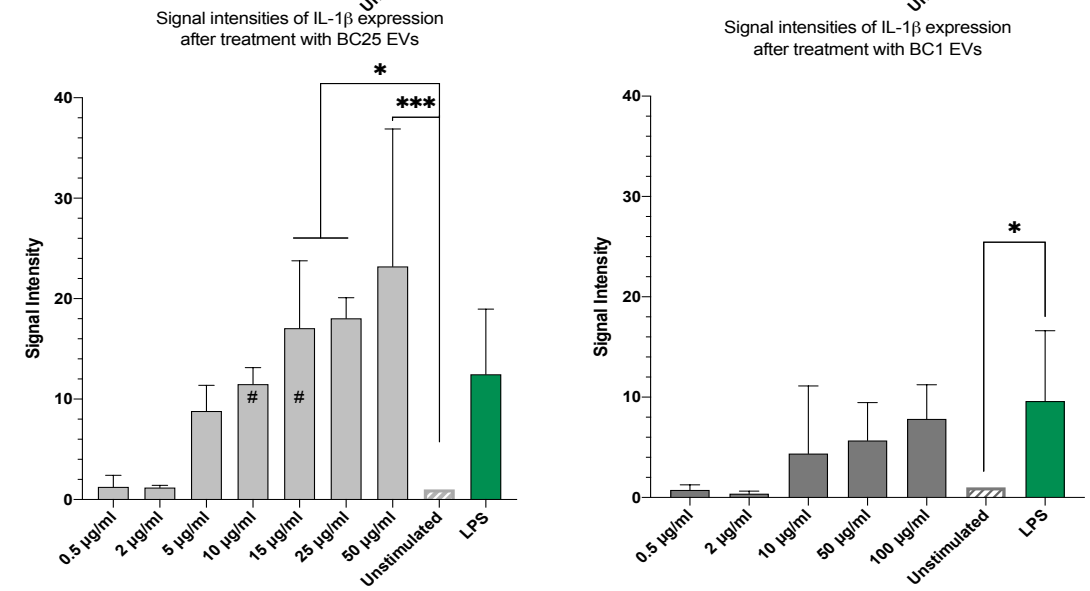
Signal intensities of IL-1β expression after treatment with BC25 EVs
Signal Intensity
Signal intensities of IL-1β expression after treatment with BC1 EVs

C)

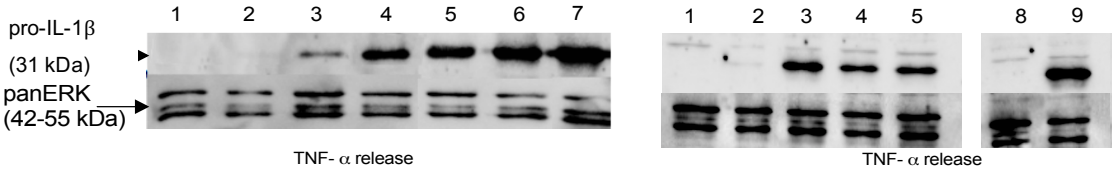
pro-IL-1β
(31 kDa)
panERK
(42-55 kDa)

D)

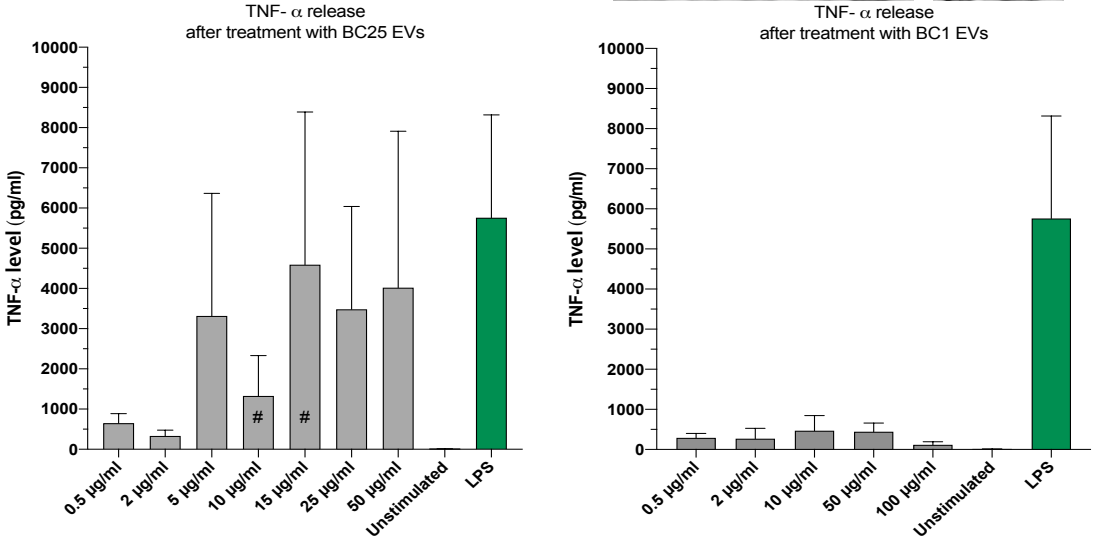
TNF- α release after treatment with BC25 EVs
TNF-α level (pg/ml)
TNF- α release after treatment with BC1 EVs

Fig. 18: Cytotoxic effects and response of immuno-stimulatory markers released upon EV stimulation from *B. cereus* strains BC25 and BC1. Panel **(A)** illustrates LDH release and panel **(B)** shows band intensities of IL-1β western blot. Western blots were performed in unicates. A representative western blot of pro-IL-1β expression is shown in panel **(C)** together with the expression of the housekeeping protein panERK. Samples were stimulated with following EV concentrations: lane 1 with 0.5 µg/ml, lane 2 with 2 µg/ml, lane 3 with 5 µg/ml, lane 4 with 10 µg/ml, lane 5 with 15 µg/ml, lane 6 with 25 µg/ml and lane 7 with 50 µg/ml. Accordingly, following BC1 EV concentrations were used: lane 1 with 0.5 µg/ml, lane 2 with 2 µg/ml, lane 3 with 10 µg/ml, lane 4 with 50 µg/ml, lane 5 with 100 µg/ml. Lane 8 depicts unstimulated cells and lane 9 cells stimulated with 100 ng/ml LPS. Panel **(D)** shows TNF-α expression. Three independent experiments were performed, stimulations marked with # were only performed twice. Quadruplicates were used to measure LDH release **(A),** unicates were used for western blotting **(B)** and duplicates were used for ELISA **(D)**. Error bars represent means and standard deviation. Samples were compared to unstimulated cells with a One-way ANOVA with Dunnett's multiple comparison test (*P < 0.05, ***P < 0.001, ****P < 0.0001).

The roles of NheB and SMase were assessed by application of EVs of the isogenic mutants of BC25 and BC1. As depicted in Fig. 12, the phospholipid levels were normalized to the parent strain. Again, LDH release was measured as a marker for cytotoxicity (Fig. 19A), and intracellular pro-IL-1β and TNF-α release as a immunostimulatory marker (Fig. 19B-C).

Comparing the cytotoxicity levels of cells stimulated with EVs and unstimulated cells only 5 µg/ml and 10 µg/ml EVs purified from BC25 (49.28 % / 57.38 % Cytotoxicity, respectively) and BC25*Δsph* (21.47 % / 50.53 % Cytotoxicity, respectively), exhibited significant cytotoxic effects. All other conditions, BC25*ΔnheBCΔsph* (5.784 % / 5.774 % Cytotoxicity, respectively), BC25*ΔnheBC* (5.152 % / 4.804 % Cytotoxicity, respectively) and BC1*ΔplcR* (6.731 % / 8.035 % Cytotoxicity, respectively), showed no significant differences towards unstimulated cells (Fig. 19A).

Stimulation with EVs derived from BC25*Δsph* and BC1*ΔplcR* provoked a strong pro-IL-1β response. However, stimulation with BC25*ΔnheBC* and BC25*ΔnheBCΔsph* (10 µg/ml) also triggered pro-IL-1β release although weaker (Fig. 19B)

TNF-α responses were very strong in all conditions except BC25*ΔnheBCΔsph* (5 and 10 µg/ml). However the similar TNF-α levels, ranging from 0.91 to 0.954 ng/ml, suggest that the maximal saturation level was reached (Fig. 19C).

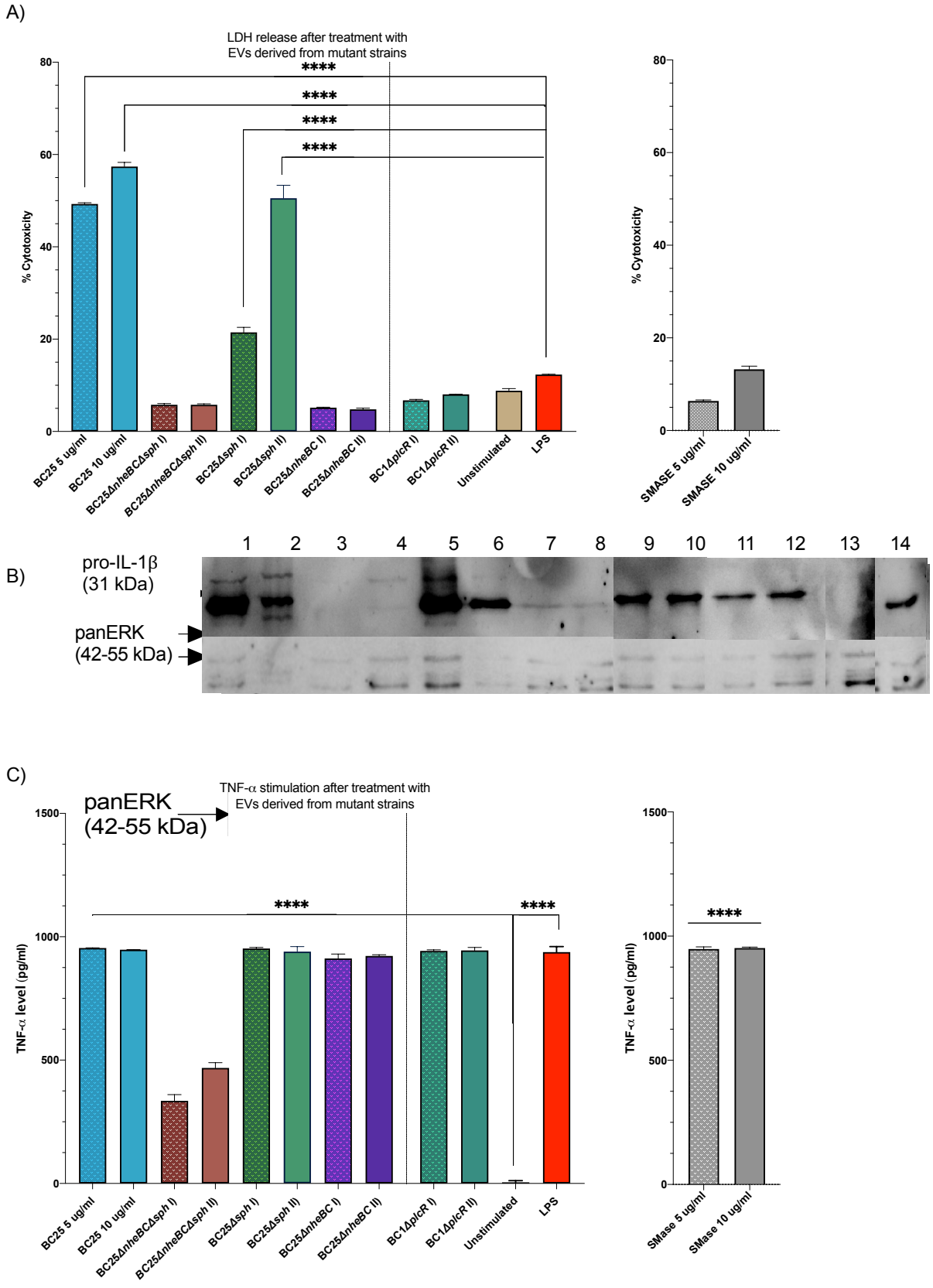

Fig. 19: Cytotoxic effects and response of immuno-stimulatory markers released upon EV stimulation. In panel **(A)** LDH release and in panel **(B)** a representative western blot for pro-IL-1β expression and the according panERK expression is displayed. Lane 1 and 2 were stimulated with BC25 EVs (5 and 10 µg/ml), lane 3 and 4 with BC25*ΔnheBCΔsph* EVs, lane 5 and 6 with BC25*ΔnheBC* EVs, lane 7 and 8 with BC25*Δsph* EVs, lane 9 and 10 with *BC1ΔplcR EVs,* Lane 11 and 12 were stimulated with plain SMase. Lane 13 shows untreated cells, and lane 14 cells treated with the positive control (100 ng/ml LPS). *BC1* EVs were out of stock, and therefore note applied. Lanes I) and II) were stimulated with the amount of EVs corresponding to phospholipid content in 5 µg

and 10 µg in BC25, and 50 µg and 100 µg in BC1 EVs. The amount of SMase used, was adjusted to the SMase activity of 5 µg and 10 µg BC25. Panel **(C)** shows TNF- α expression. A single experiment was performed, duplicates were used to measure LDH release **(A),** unicates were used for western blotting **(B)** and duplicates were used for ELISA **(C).** Error bars represent arithmetic means and standard deviation. Samples were compared to unstimulated cells with a One-way ANOVA with Dunnett's multiple comparison test (*P < 0.05, ****P < 0.0001).

4. Discussion

4.1. Characterisation of *B. cereus* EVs

The secretion of EVs was already elaborately studied in EVs derived from mammalian cells. However, the secretion of such structures seems to be a ubiquitous process, as it was shown for several fungal and bacterial species, for example, *Cryptococcus neoformans*, *S. aureus*, *B. subtilis* and *B. anthracis* (Brown *et al*., 2014; Rivera *et al*., 2010; Rodrigues *et al.*, 2008; Schlatterer *et al.*, 2018). It is therefore not only restricted to Gram-negative bacteria, as previously thought, but also occurs in fungi and in Gram-positive bacteria. This current study characterises an additional Gram-positive germ able to secrete EVs.

As shown in the work of Jeßberger and co-workers (Jeßberger *et al*., 2017), protein secretion and toxin gene transcription is accelerated when bacteria are cultivated under simulated intestinal conditions, with the presence of Caco-2 cell-secreted factors in the medium. Our work demonstrated that also EV production is triggered by cultivation under host-mimicking conditions. In accordance to previous work, we noticed decreased growth rates of BC25 cultured in cRPMI (Jeßberger *et al.*, 2017). The protein amount of EVs was strongly dependent bacterial growth phase, which suggests that EVs secretion is regulated by growth phase-dependent mechanisms. EVs were detectable from OD_{600} = 0.79 (mid exponential phase) onwards, but not in the early growth phase OD_{600} = 0.39.

Immunoblot analyses of the EVs, isolated by size exclusion centrifugation, revealed that the EVs contain NheB and Smase, which have been recently been reported to represent important markers for enteropathogenicity of *B. cereus* (Jeßberger, Kranzler *et al*., in press). This is in line with data from vesicle studies of Buchacher *et al*., which showed that NheA is mainly found in the flow-through while NheB is mainly found in the EV fraction (Buchacher *et al*., in preparation). By immunoblotting PI-phospholipase C and collagenase A were only detectable in the flow-through but not in the EVs. However, a collagenase (53 % coverage) was found in frame of the proteome analysis of EVs, which might be explained by the presence of various collagenases in *B. cereus* (Abfalter *et al*., 2016), one in the flow through targeted by the ColA antibody used for immunoblotting and another, which is not recognized be the ColA antibody used for immunoblotting, in the EVs. Thus, further studies are necessary to dissect the role of the diverse collagenases of B. cereus for its pathogenicity.

Moreover, NheC is exclusively detected in the EV fraction. This indicates a regulated transport mechanism of the Nhe components into the environment and the EVs, as it could also shown by this present work that NheB was found in both fraction and NheA exclusively in the vesicle-free supernatant. However, the presence of NheB and NheC in EVs might

illustrate a protection mechanism, either to protect the protein from extracellular proteases, or to ensure the ratio of 10:10:1 = NheA, NheB, NheC *(Lindbäck et al.,* 2004, 2010)

In addition, we observed that EVs of BC25*Δsph* expressed higher levels of NheB, and BC25*ΔnheBC* expressed higher amounts of SMase than the parent strain BC25, which might reflect a higher uptake of SMAse or NheB in the respective mutant to compensate for the loss of the other virulence factor. Indeed, it has been shown recently, that NheB and SMase are the key indicator for enterotoxicity of *B. cereus* (Jeßberger, Kranzler *et al*, in press) and act in a synergistic manner (Doll *et al*., 2013). However further studies will be necessary to fully decipher the roles as a virulence factor in EVs.

Proteomic studies of the EVs showed a versatile protein composition, including proteins involved in fatty acid, carbohydrate and amino acid metabolism, ABC transporters and proteins associated with bacterial motility. In line with the present study, this protein diversity was also observed in EVs isolated from *B. anthracis*, *S. aureus* and *C. perfringens* (Lee *et al*., 2009; Rivera *et al.*, 2010; Yanlong *et al*., 2014).

The identified proteins of *B. cereus* EVs also comprise canonical intracellular metabolic enzymes, such as glucose-6-phosphate isomerase, which is essential for gluconeogenesis. There might be a link to the so-called ‘moonlighting proteins’. These are proteins that elicit more than two functions, are often located on the cell surface or extracellularly and often interfere with the hosts’ organism by binding to proteins (Amblee & Jeffery, 2015; Franco *et al*., 2018; for review see Henderson & Martin, 2011; Jeffery, 2019), For the above mentioned enzyme, it was shown to act as a neuroleukin, promoting survival of motor and sensory neurons (Faik *et al*., 1988; Read *et al*., 2001).

As the secretion of extracellular vesicles appears to be a ubiquitous process, the structural morphology of the EVs of different bacterial and fungal species is akin to those of *B. cereus* (Rivera *et al*., 2010; Rodrigues *et al*., 2008; Schlatterer et al., 2018). Vesicles derived from Gram-negative bacteria are described as spherical structures ranging from 20 to 400 nm in diameter (for review see Toyofuku *et al*., 2019). These sizes also reflect those, found in Gram-positive bacteria, and also resemble our findings in *B. cereus*, which have diameters from 20 to 290 nm, although single EVs were found to be larger than 290 nm. The similar dimensions of Gram-positive, Gram-negative and fungal vesicles might point towards the existence of a conserved mechanism for vesiculogenesis. However, the comparable visual nature of EVs might also reflect basic biophysical mechanisms underlying liposome formation.

Electron microscopy revealed that the EVs of *B. cereus* are not a uniform population. Electron dense (dark) and electron light (bright) EVs, and further structures, such as nested EVs, were present. EVs isolated from BC25 and BC1*ΔplcR* were mainly found to be either

dark or bright. Rodrigues and co-workers (Rodrigues *et al*., 2008) also identified dark EVs and bright EVs originating of *Cryptococcus neoformans*. The significant differences in size between bright and dark EVs might reflect a different mechanism of vesiculogenesis and/or transport. Dark EVs were approximately 73.68 nm in diameter, with maximal sizes of 180 nm, whereas bright EVs were two to three times larger, with maximal diameters of 320 nm.

As in BC1 EVs, which contained a low amount of proeins, only bright structures were observed, it is tempting to speculate that especially dark EVs are filled with protein. This hypothesis is fostered by the results from SDS Page, where only two bands were detected, and the low amount of proteins (n=212) identified by Exactive Orbitrap LC-MS/MS. In contrast, SDS PAGE analysis of BC25 EVs revealed more than fifteen protein bands and more than 400 identified proteins by Orbitrap LC-MS/MS.

Contrary to dark EVs, nested EVs could be visualized in every strain, despite BC1. It can be excluded that these images are artefacts, as the diameter of the outmost EV exceeds 70 nm, the thickness of the ultra-thin slice. So far, it can only be speculated how these structures arise. These structures might develop during incomplete budding of the EVs, but also could also reflect a stress response to environmental conditions. This work presents the first report of such structures, hence further studies will be needed to elucidate the role and potential functions of these structures. In addition, the underlying reasons for formation of other structures, like nested EVs, the EVs secreted by BC25*ΔnheBCΔsph* – which showed a prominent dark cloud around the membrane –, and the EVs secreted by BC1*ΔplcR,* still remain elusive and needs further investigation.

It has also been reported that EVs of *L. monocytogenes* mutants exhibited a deformed appearance (Lee *et al*., 2013). Intriguingly, pathogenic *E. coli* produced more OMVs than non-pathogenic *E. coli* (Wai *et al*., 1995). The loss of YfgL, a lipoprotein important for the synthesis and/or degradation of peptidoglycans, causes reduced production of OMVs in invasive *E. coli* (Rolhion *et al*., 2005). Although these findings were obtained from Gram-negative EVs, similar findings were also found in Gram-positive *L. monocytogenes*. A general stress transcription factor, termed σB, which is involved in host invasion, may be related to increased production of EVs to promote survival under harsh environments or during infection (Lee *et al*., 2013).

The fibrous structures, observed in the EV fractions of *B. cereus* by TEM fits to those of *B. subtilis* flagella (Mukherjee & Kearns, 2014). This hypothesis is also fostered by the results of immunoblotting, where Flagellin could be detected in the EV fraction. Moreover, proteomic analysis showed that flagellin is the most abundant protein and it was detected in each EV fraction. It is tempting to speculate that due to the petrichous flagellation of *B. cereus* and the numerous centrifugation steps during EV isolation, the flagella break down during sample

preparation and is therefore found in the EV fraction. Nevertheless, Salvetti and co-workers (Salvetti *et al.,* 2007) also showed that flagella-deficient *B. cereus* secreted less extracellular proteins. It was further shown that knockout FlhF – a transcriptional regulator of the flagellin-harboring *fla* operon –, resulted in diminished expression of SMase, ColA, and PI-PLC (Mazzantini *et al.,* 2016). In addition, Hayashi and co-workers (Hayashi *et al*., 2001) showed that bacterial flagella are potent TLR5 stimulators. There, TLR5 stimulation resulted in the same expression patterns as shown in our work (TNF-α and pro-IL-1β). However, due to the lack of pro-IL-1β and TNF-α expression in cells stimulated with EVs derived from BC25*ΔnheBCΔsph* and BC1, respectively, the immune-stimulatory effect of the EV co-incubation can be clearly assigned to those of the vesicular structures and not to the flagellar fragments.

As variable levels of phospholipids were detected in the EVs of the different B. cereus strains, it could be assumed that the EV membrane is composed of different components varying between strains. Measurements by Fourier-transform infrared spectroscopy might help to address this question. Moreover, staining with specific fluorescent membrane dyes, as used by Schlatterer and colleagues might provide suitable tools to promote the understanding of the EV composition (Schlatterer *et al*., 2018).

4.2. Roles of *B. cereus* EVs as a novel virulence factor

The link between extracellular vesicles and disease was already extensively elaborated in mammalian cells (for review see Tkach & Thery, 2016). However in the last decade, EVs secreted from bacteria also gained importance as a novel virulence factor to consider. The so far most extensively studied EVs from Gram-positive bacteria, are EVs derived from *S. aureus.* According to the current state of knowledge, these EVs have crucial roles in methicillin-resistant *S. aureus* (MRSA) biofilm formation, in the delivery of virulence factors to the host and in several diseases, such as atopic dermatitis-like inflammation (Andreoni *et al*., 2019; Gurung *et al*., 2011; Hong *et al*., 2011). In addition, thymol, which is commonly used as an anti-microbial, anti-cancerous and anti-inflammatory substance, might attenuate the production of EVs derived from *S. aureus* (Aeschbach *et al*., 1994; Il *et al*., 2019; Wan *et al*., 2017).

To elucidate the role of EVs in pathogenicity of B. cereus, a established model for sepsis was used. The results of this work strongly suggest that *Bacillus cereus* EVs exhibits both cytotoxic and immunostimulatory properties. Cytotoxicity mediated by EVs purified from BC1 and BC25 differed, due to the respective strain background, we could stimulate intracellular TNF-α and pro-IL-1β response release by application of both strains. As BC25*ΔnheBC* EVs were less cytotoxic to the cells than BC25*Δsph* EVs, it is concluded that the main cytotoxic component of the EVs are the enterotoxins NheB and NheC. It was previously shown that

NheB and NheC are important for membrane binding and complex formation, whereas NheA functions as the final binding unit to complete the membrane pore (Heilkenbrinker *et al*., 2013; Lindbäck *et al*., 2010). Fagerlund and colleagues (Fagerlund *et al.,* 2008) demonstrated the total loss of cytotoxicity by application of BC25*ΔnheBC* supernatant to Vero cells. A similar effect by application of mutant BC25*ΔnheBC* EVs to BMDMs was observed in this work. Therefore it can be concluded that the total loss of cytotoxicity in the *nheBC* mutant EVs is due to the absence of NheB and NheC, and NheA alone cannot act in a cytotoxic manner (Lindbäck *et al*., 2004). Interestingly, EVs isolated of BC25*Δsph* were less cytotoxic than the EVs from its parental strain BC25. This supports the synergistic interactions between Nhe and SMase, which were previously shown by Doll and colleagues (Doll *et al*., 2013).

Treatment with purified SMase (0.5 Units/ml) resulted in higher cytotoxicity levels as observed in cells treated with BC25*ΔnheBC* EVs. This result shows that the amount of SMase within the EVs, is sufficient to confer cytotoxicity, and further advocates the importance of NheB and NheC for EV mediated cytotoxicity. The EVs derived from the double mutant could not stimulate expression of pro-IL-1β, whereas TNF-α was stimulated. All other strains could induce expression of both pro-inflammatory cytokines, possibly due to the synergistic interactions of NheBC and SMase. Oda and colleagues proposed central roles of SMase for the onset of *B. cereus* infections, as peritoneal treatment with SMase resulted in reduced phagocytosis and release of H_2O_2 (Oda *et al*., 2012). The observations by this study suggest the importance of considering EV-mediated actions in the pathogenesis of *B. cereus* and might provide auxillary insight into the onset of non-gastrointestinal related diseases, such as sepsis, endophtalmitis and endocarditis (Bottone, 2010; Messelhäußer & Ehling-Schulz, 2018; Oda *et al.,* 2012).

As shown in the current work, the toxins, nheBC and SMase, which represent an important virulence factor in *B. cereus (*Jeßberger, Kranzler *et al,* in press*)* can be found in the EV fraction, indicating that they are packed in and transported extracellularly by vesicles to the target host cells. It can be speculated that they release their toxic potential by fusioning of EVs with the host cell. Moreover, it is hypothesized that EVs secreted by *B. cereus* could illustrate some kind of mimickry-like strategy to invade the host organism. By secretion of these structures, containing potential moonlighting proteins and virulence factors, the host's first line of defence might be redirected from the bacterial cell and focuses to the combating of the EVs. However, it is clear that these hypotheses need systematic verification and this thesis only offers limited, however, novel insight.

4.3. Conclusion

In conclusion, the findings of this thesis contribute to a better understanding of EV-mediated toxicity and vesiculogenesis in Gram-positive bacteria. It not only identifies a Gram-positive organism capable to secrete EVs, but also assigns putative roles of EVs.

It was demonstrated that EVs derived from *B. cereus* are cytotoxic against BMDM and exhibit immune-stimulatory properties. Moreover, our results further confirm the synthesis and production of vesicular structures in Gram-positive bacteria. In addition, it was proved that EVs isolated of *B. cereus* structures transport biologically active toxins and stimulate pro-inflammatory cytokines. Consequently, vesicle production can be associated with the delivery of virulence components. Up to now, the delivery of virulence factors was shown for several species, for example *E. coli, Pseudomonas aeruginosa, C. neoformans, Helicobacter pylori, B. anthracis and S. aureus* (Bauman & Kuehn, 2009; Fiocca *et al.,* 1999; Mcbroom *et al.,* 2006; Rivera *et al.,* 2010; Rodrigues *et al.,* 2008; Schlatterer *et al.,* 2018).

Summing up, this thesis constitutes an important pioneer work for future analyses with EVs of *B. cereus*.

4.4. Outlook

During inoculation in different media and at different time points, variable EV protein patterns was observed in inoculation in LB, whereas inoculation in cRPMI was rather constant. This indicates that protein expression is depending on the bacterial growth phase and also observable in EVs. However, to further assess the biological functions of EVs, sampling at additional time points should be considered. Furthermore, since the transcription of *nheB* is enhanced during incubation in cRPMI, it is tempting to speculate that vesiculogenesis is linked to the enhanced transcription rate (Jeßberger *et al*., 2017). Further studies, investigating the effects of host mimicking and other conditions, might reveal the real cytotoxic and inflammatory potential of EV structures.

Recently, it was discovered that *B. cereus* can switch to a subpopulation called small colony variants (SCVs), a phenotype less susceptible to antibiotics and more persistent for survival within the host (Frenzel, Kranzler *et al*. 2015). The cytotoxic and infectious potential of this novel lifestyle was examined using *Galleria mellonella* as a model organism (Frenzel, Kranzler *et al*., 2015). In addition, this insect is extensively used as a model organism to assess infectious potential of *B. cereus* (Frenzel *et al.*, 2012; Ollinger *et al*., 2009; Ramarao *et al*., 2012, Mazzantini *et al*., 2016). Injection of EVs to this organism might lead to further insights into the pathogenic potential of EVs.

Moreover, Oda and co-workers showed that intraperitoneal injection of SMase, purified from pathogenic and non-pathogenic *B. cereus* strains, inhibited macrophage activation (Oda *et*

al., 2012). It is therefore tempting to speculate that this mechanism is also activated in EVs containing SMase and a crucial factor to contemplate when evaluating non-GI related diseases provoked by *B. cereus.*

Therefore, the final step to investigate the importance of EVs as a novel virulence factor or vaccine platform may be the application to a mouse model. Intramammal, intratracheal and intraperitoneal application of EVs were already conducted to study specific pathogenic properties (Prados-Rosales *et al*., 2011; Tartaglia *et al*., 2018; Wang *et al*., 2019). Wang and co-workers showed that OMVs released from Gram-negative bacteria have crucial roles in the onset of disseminated intravascular coagulation, a fatal complication in sepsis leading to oxygen deprivation and ultimately to multiple organ failure (Wang *et al*., 2019; Levi & Cate, 1999). In addition, immunization studies in mice are currently used to evaluate the use of bacterial vesicles as a vaccination platform, in both Gram-negative and Gram-positive bacteria-derived vesicles (Liu *et al*., 2018; Wang *et al*., 2018).

Thus, application of EVs from different *B. cereus* strains to a mouse model will provide insight into EV mediated pathogenicity. Moreover, the further use of genetic modified mice, for example the knock-out of specific toll-like receptors will elucidate the pathways triggered by application of EVs and also clarify the role of SMase within the EVs. However, also the application of heat-inactivated or sonicated EVs in *in vitro* and *in vivo* models will uncover more details in EV-mediated cytotoxicity and the role of the EV membrane. Finally, further studies emphasising on proteins with possible ‘moonlighting activity’ might shed some light on pathogenic properties.

Taken together all aspects of this thesis, this opens a panoply of research questions to be followed up and an emerging field in combating *B. cereus* related diseases.

5. Zusammenfassung

Bacillus cereus ist ein grampositives, stäbchenförmiges Bakterium zugehörig der Gattung Bacillus. Durch die ubiquitäre Präsenz in der Natur wird dieser Keim auch in vielen verschiedenen Nahrungsmitteln gefunden. Das pathogene Spektrum von *B. cereus* ist sehr breit und reicht von probiotischen Stämmen bis zu hochletalen und toxischen Stämmen. Trotzdem ist er weltweit als Lebensmittelvergiftung verursachender Krankheitserreger bekannt. Die von *B. cereus* verursachten gastrointestinalen Erkrankungen haben normalerweise eine milde Prognose, es wurden jedoch Fälle mit tödlichem Ausgang gemeldet. In den letzten Jahren wurde die Beteiligung von *B. cereus* auch bei Erkrankungen erkannt, die nicht im Zusammenhang mit Lebensmittelvergiftungen und dem Verdauungstrakt stehen, wie zum Beispiel Sepsis, Endophalmitis und Endokarditis.

In dieser Arbeit wurde ein neuer Virulenzfaktor identifiziert und charakterisiert. Die Eigenschaften dieses Faktors wurden unter Verwendung eines Westernblot- und Proteom-Ansatzes bewertet. Darüber hinaus wurde die biologische Aktivität durch Anwendung auf eine primäre Zellkultur unter Verwendung von aus Knochenmark stammenden Makrophagen als Modell evaluiert.

Wir haben gezeigt, dass die Produktion dieses Faktors durch Verwendung von Medium gesteigert werden kann, das zuvor in Medium mit Caco-2 Zellen konditioniert wurde. Darüber hinaus war die Produktion dieses Faktors unabhängig vom Transkriptionsregulator *plcR* und den Virulenzgenen *nheB*, *nheC* und *sph*. Die Anwendung dieses Virulenzfaktors wirkte dosisabhängig und konnte die Expression von pro-IL-1β und TNF-α stimulieren. Diese Ergebnisse deuten darauf hin, dass dieser Faktor möglicherweise zu Erkrankungen beiträgt die nicht zu dem klassischen Krankheitsbild von *B. cerues* gehören. Da diese Arbeit die Erst-Charakterisierung dieses Faktors darstellt, sind weitere Studien in *in vivo* Modellen nötig, um das weitere immunogene und pathogene Potential dieses Faktors zu bestimmen.

6. Summary

B. cereus is a Gram-positive rod, which is world-wide associated as an emerging human food-borne pathogen. The pathogenic range of B. cereus is very broad, ranging from probiotic strains, to highly lethal and toxic strains. The GI-related diseases caused by *B. cereus* usually have a mild prognosis, but cases with fatal outcome have been reported. In recent years the participation of *B. cereus* was also recognized in non-GI related diseases for instance, sepsis, endocarditis and endophalmitis.

In regard to this, this work identified and characterized a novel virulence factor. The properties of this factor were evaluated using a western blot and proteomic approach. Furthermore, the biological activity was assessed by application on a primary cell culture, using bone-marrow-derived macrophages as a model.

We showed that using medium, which was prior conditioned with Caco-2 cells, could enhance the production of this factor. Moreover, the production of this factor was independent from the transcription regulator *plcR,* and the virulence genes *nheB*, *nheC* and *sph*. The application of this factor acted in a dose-depended fashion and was able to stimulate the expression of pro-IL-1β and TNF-α. These results signify that this factor might contribute to non-GI related diseases, for example sepsis, but also might influence the onset of food-poisoning symptoms. However, further studies in *in vivo* models are crucial to fully evaluate the immunostimulatory and pathogenic potential.

7. Indexes

7.1. Index of figures

7.2. Index of tables

7.3. Abbrevations

AFM	Atomic force microscopy
APS	Ammonium persulfate
BMDMs	Bone-marrow-derived macrophages
BSA	Bovine serum albumine
CGY broth	Casein glucose yeast broth
cMedium	conditioned DMEM Medium (with L929 cells)
cRPMI	conditioned RPMI Medium (with Caco-2 cells)
Cyt K	Cytotoxin K
DMEM	Dulbeccos's modified Eagle's medium
DMSO	Dimethyl sulfoxide
DTT	Dithiothreitol
ECM	Extracellular matrix
EtOH	Ethanol
EVs	Extracellular vesicles
FBS	Fetal bovine serum
GCSF	Granulocyte colony stimulating factor
GI tract	Gastrointestinal tract
Hbl	haemolysin BL
IgE	Imunoglobulin E
IL	Interleukin
ISEV	International society for extracellular vesicles
lEVs	large EVs
LB	Lysogeny broth
LDH	Lactate dehydrogenase

LPS	Lipopolysaccharide
LTA	Lipoteichonic acids
OMVs	Outer membrane vesicles
MAPK	Mitogen activated protein kinase
MetOH	Methanol
mEVs	medium EVs
MISEV	Minimial information for studies on extracellular vesicles
MRSA	Methicillin-resistant *S. aureus*
MyD88	Myeloid differentiation primary response 88
Nhe	Non-haemolytic toxin
NFkB	Nuclear factor kappa light chain enhancer of activated B-cells
PA	Phosphatidylethanolamine
PBS	Phosphate buffered saline
PC	Phosphatidylcholine
PC Agar	Plate count agar
PC-PLC	Phosphatidylcholine specific PLC
PI-PLC	Phosphatidylinositol specific PLC
PLC	Phospholipase C
plcR	Phospholipase C regulator
PMSF	phenylmethylsulfonyl flouride
PS	Phosphatidylserine
SDS	Sodium dodecyl sulfate
sEVs	small EVs
SMase	Sphingomyelinase
TCA	Trichloroacetic acid
TFA	Trifluoroacetic acid
TH_{17}	T-helper cells 17
TEM	Transmission electron microscopy
TLR	Toll like receptor
Temed	Tetramethylethylendiamin
TNF	Tumor necrosis factor
WTAs	Wall teichonic acids

8. References

Abfalter, C. M., Schönauer, E., Ponnuraj, K., Huemer, M., Gadermaier, G., Regl, C., … Wessler, S. (2016). Cloning , Purification and Characterization of the Collagenase ColA Expressed by Bacillus cereus ATCC 14579. *Plos ONE*, *11*(9), 1–19. https://doi.org/10.1371/journal.pone.0162433

Aeschbach, R., Lölinger, J., Scott, B., Murcia, A., Butler, J., Halliwell, B., & Aruoma, O. (1994). Antioxidant actions of thymol, carvacrol, 6-gingerol, zingerone and hydroxytyrosol. *Fd Chem Toxic*, *32*(I), 31–36.

Agata, N., Ohta, M., Mori, M., & Isobe, M. (1961). A novel dodecadepsipeptide, cereulide, is an emetic toxon of Bacillus cereus. *FEMS Microbiology Letters*, *129*, 17–20. Retrieved from https://attachment.outlook.office.net/owa/jazminvaleriano@hotmail.com/service.svc/s/GetFileAttachment?id=AQMkADAwATY3ZmYAZS1jOTkAYy1lMWIxLTAwAi0wMAoARgAAA8kybMmZw%2B1PigImBiTGWb8HADhlo3wuKERGuW5ksIxez68AAAIBDAAAADhlo3wuKERGuW5ksIxez68AAAKXbgAAAAESABAAPp1V

Agata, N., Ohta, M., & Yokoyama, K. (2002). Production of Bacillus cereus emetic toxin (cereulide) in various foods. *International Journal of Food Microbiology*, *73*(1), 23–27. https://doi.org/10.1016/S0168-1605(01)00692-4

Ago, H., Oda, M., Takahashi, M., Tsuge, H., Ochi, S., Katunuma, N., … Sakurai, J. (2006). Structural Basis of the Sphingomyelin Phosphodiesterase Activity in Neutral Sphingomyelinase from Bacillus cereus *. *The Journal of Biological Chemistry*, *281*(23), 16157–16167. https://doi.org/10.1074/jbc.M601089200

Albuquerque, P. C., Nakayasu, E. S., Rodrigues, M. L., Frases, S., Casadevall, A., Zancope-Oliveira, R. M., … Nosanchuk, J. D. (2008). Vesicular transport in Histoplasma capsulatum: An effective mechanism for trans-cell wall transfer of proteins and lipids in ascomycetes. *Cellular Microbiology*, *10*(8), 1695–1710. https://doi.org/10.1111/j.1462-5822.2008.01160.x

Alonso, A., Biomembranas, G., Asociada, U., Bioquı, D. De, & Uni, V. (1998). Phospholipase C Hydrolysis of Phospholipids in Bilayers of Mixed Lipid. *Biochemistry*, *37*, 11621–11628.

Altindis, E., Fu, Y., & Mekalanos, J. J. (2014). Proteomic analysis of Vibrio cholerae outer membrane vesicles. *PNAS*, E1548–E11556. https://doi.org/10.1073/pnas.1403683111

Amblee, V., & Jeffery, C. J. (2015). Physical Features of Intracellular Proteins that Moonlight on the Cell Surface. *PLoS ONE*, *10*(6), 1–16.

https://doi.org/10.1371/journal.pone.0130575

Andreoni, F., Toyofuku, M., Menzi, C., Kalawong, R., & Shambat, M. (2019). Antibiotics stimulate formation of vesicles in staphylococcus aureus in both Phage-Dependent and -Independent Fashions and via different routes. *Antimicrobial Agents and Cemotherapy*, *63*(2), 1–10.

Aronson, A. I., & Shai, Y. (2001). Why Bacillus thuringiensis insecticidal toxins are so e ¡ ective : unique features of their mode of action. *FEMS Microbiology Letters*, *195*, 1–8.

Ash, C., Farrow, J. A. E., Dorsch, M., Stackebrandt, E., & Collins, M. D. (1991). Comparative Analysis of Bacillus-Anthracis, Bacillus-Cereus, and Related Species on the Basis of Reverse Transcriptase Sequencing of 16S rRNA. *Int J Syst Bact*, *41*, 343–346.

Auwera, G. A. Van Der, Timmery, S., Hoton, F., & Mahillon, J. (2007). Plasmid exchanges among members of the Bacillus cereus group in foodstuffs. *Internatinal Journal of Food Microbiology*, *113*, 164–172. https://doi.org/10.1016/j.ijfoodmicro.2006.06.030

Bauman, S. J., & Kuehn, M. J. (2009). Pseudomonas aeruginosa vesicles associate with and are internalized by human lung epithelial cells. *BMC Microbiology*, *9*(26), 1–12. https://doi.org/10.1186/1471-2180-9-26

Beecher, D. J., & MacMillan, J. D. (1991). Characterization of the components of hemolysin BL from Bacillus cereus. *Infection and Immunity*, *59*(5), 1778–1784.

Beecher, D. J., Olsen, T. W., Somers, E. B., & Wong, A. M. Y. C. L. (2000). Evidence for Contribution of Tripartite Hemolysin BL , Phosphatidylcholine-Preferring Phospholipase C , and Collagenase to Virulence of Bacillus cereus Endophthalmitis. *Infection and Immunity*, *68*(9), 5269–5276.

Beecher, D. J., Wong, A. C. L., & Drive, W. (2000). Cooperative , synergistic and antagonistic haemolytic interactions between haemolysin BL , phosphatidylcholine phospholipase C and sphingomyelinase from Bacillus cereus. *Microbiology*, *146*, 3033–3039.

Berman, E. R. (1991). Biochemistry of the Eye. In *Biochemical Education* (Vol. 19).

Birnbaum, D., Bertucci, F., & Sabatier, R. (2019). Liquid Biopsies for Ovarian Carcinoma : How Blood Tests May Improve the Clinical Management of a Deadly Disease. *Cancers*, *11*(774), 1–23.

Bitto, N. J., Chapman, R., Pidot, S., Costin, A., Lo, C., Choi, J., … Ferrero, R. L. (2017). Bacterial membrane vesicles transport their DNA cargo into host cells. *Scientific Reports*, (November 2016), 1–11. https://doi.org/10.1038/s41598-017-07288-4

Bos, M. P., Robert, V., & Tommassen, J. (2007). Biogenesis of the Gram-Negative Bacterial

Outer Membrane. *Annual Review of Microbiology*, *61*(1), 191–214. https://doi.org/10.1146/annurev.micro.61.080706.093245

Bosmann, M., Russkamp, N., Strobl, B., Roewe, J., Balouzian, L., Pache, F., … Ward, P. (2014). Interruption of macrophage-derived IL-27 (p28) production by IL-10 during sepsis requires STAT3 but not SOCS3. *Journal of Immunology*, *193*(11), 5668–5677. https://doi.org/10.4049/jimmunol.1302280.Interruption

Bottone, E. J. (2010). Bacillus cereus, a volatile human pathogen. *Clinical Microbiology Reviews*, *23*(2), 382–398. https://doi.org/10.1128/CMR.00073-09

Brown, L., Kessler, A., Cabezas-Sanchez, P., Luque-Garcia, J. L., & Casadevall, A. (2014). Extracellular Vesicles Produced by the Gram-positive Bacterium Bacillus subtilis are Disrupted by the Lipopeptide Surfactin. *Molecular Microbiology*, *93*(1), 183–198. https://doi.org/10.1111/mmi.12650.Extracellular

Brown, L., Wolf, J. M., Prados-Rosales, R., & Casadevall, A. (2015). Through the wall: Extracellular vesicles in Gram-positive bacteria, mycobacteria and fungi. *Nature Reviews Microbiology*, *13*(10), 620–630. https://doi.org/10.1038/nrmicro3480

Buchacher, *et al.* in preparation

Carlson, C. R., & Caugant, D. A. (1994). Genotypic Diversity among Bacillus cereus and Bacillus thuringiensis Strains. *Applied and Environmental Microbiology*, *60*(6), 1719–1725.

Claus, D., & Fritze, D. (1989). Taxonomy of Bacillus. In *Bacillus. Biotechnology Handbooks*.

Dean, S. N., Leary, D. H., Sullivan, C. J., Oh, E., & Walper, S. A. (2019). Isolation and characterization of Lactobacillus -derived membrane vesicles. *Scientific Reports*, (August 2018), 1–11. https://doi.org/10.1038/s41598-018-37120-6

Deatheragea, B. L., & Cooksona, B. T. (2012). Membrane vesicle release in bacteria, eukaryotes, and archaea: A conserved yet underappreciated aspect of microbial life. *Infection and Immunity*, *80*(6), 1948–1957. https://doi.org/10.1128/IAI.06014-11

Dierick, K., Coillie, E. Van, Swiecicka, I., Devlieger, H., Meulemans, A., Fourie, L., … Mahillon, J. (2005). Fatal Family Outbreak of Bacillus cereus -Associated Food Poisoning Fatal Family Outbreak of Bacillus cereus -Associated Food Poisoning. *Journal of Clinical Microbiology*, *43*(8), 4277–4279. https://doi.org/10.1128/JCM.43.8.4277

Dohmae, S., Okubo, T., Higuchi, W., Takano, T., & Isobe, H. (2008). Bacillus cereus nosocomial infection from reused towels in Japan. *Journal of Hospital Infection*, 4–10. https://doi.org/10.1016/j.jhin.2008.04.014

Doll, V. M., Ehling-Schulz, M., & Vogelmann, R. (2013). Concerted Action of Sphingomyelinase and Non- Hemolytic Enterotoxin in Pathogenic Bacillus cereus. *PLoS ONE*, *8*(4), e615041-13. https://doi.org/10.1371/journal.pone.0061404

Dorward, D. W., & Garon, C. F. (1990). DNA Is Packaged within Membrane-Derived Vesicles of Gram- Negative but Not Gram-Positive Bacteria. *Applied and Environmental Microbiology*, *56*(6), 1960–1962.

Drobnik, W., Liebisch, G., Audebert, F., Fröhlich, D., Glück, T., Vogel, P., … Schmitz, G. (2003). Plasma ceramide and lysophosphatidylcholine inversely correlate with mortality in sepsis patients. *Journal of Lipid Research*, *44*, 754–761. https://doi.org/10.1194/jlr.M200401-JLR200

Ehling-Schulz, M., Fricker, M., Grallert, H., Rieck, P., Wagner, M., & Scherer, S. (2006). Cereulide synthetase gene cluster from emetic Bacillus cereus: Structure and location on a mega virulence plasmid related to Bacillus anthracis toxin plasmid pXO1. *BMC Microbiology*, *6*, 1–11. https://doi.org/10.1186/1471-2180-6-20

Ehling-Schulz, M., Fricker, M., & Scherer, S. (2004). Bacillus cereus, the causative agent of an emetic type of food-borne illness. *Molecular Nutrition and Food Research*, *48*(7), 479–487. https://doi.org/10.1002/mnfr.200400055

Ehling-Schulz, M., Knutsson, R., & Scherer, S. (2011). Bacillus cereus. In P. Fratamico, Y. Liu, & S. Kathariou (Eds.), *Genomes of Foodborne and Waterborne Pathogens* (pp. 147–164). Washington, DC: ASM Press.

Ehling-Schulz, M., Koehler, T. M., & Lereclus, D. (2019). The Bacillus cereus Group: Bacillus species with Pathogenic Potential. *Microbiology Spectrum*, *7*(3), 3–32. https://doi.org/10.1128/microbiolspec.GPP3-0032-2018.The

Ehling-Schulz, M., & Messelhäusser, U. (2014). The Genus Bacillus. In O. Omar & S. Kathariou (Eds.), *DNA Methods in Food Safety: Molecular Typing of Foodborne and Waterborne Bacterial Pathogens* (First, pp. 165–184). John Wilyes & Sons.

Ellen, A. F., Wim, Æ. S. A. Æ., Angela, H. Æ., Hobel, C. F. V, Schwarz, Æ. H., Folea, Æ. M., … Driessen, Æ. A. J. M. (2009). Proteomic analysis of secreted membrane vesicles of archaeal Sulfolobus species reveals the presence of endosome sorting complex components. *Extremophiles*, *13*, 67–79. https://doi.org/10.1007/s00792-008-0199-x

Fagerlund, A., Lindba, T., Storset, A. K., Granum, P. E., & Hardy, S. P. (2008). Bacillus cereus Nhe is a pore-forming toxin with structural and functional properties similar to the ClyA (HlyE , SheA) family of haemolysins , able to induce osmotic lysis in epithelia. *Microbiology*, (2008), 693–704. https://doi.org/10.1099/mic.0.2007/014134-0

Fagerlund, A., Ween, O., Lund, T., Hardy, S. P., & Granum, P. E. (2019). Genetic and functional analysis of the cytK family of genes in Bacillus cereus. *Microbiology*, *150*, 2689–2697. https://doi.org/10.1099/mic.0.26975-0

Faik, P., Walker, J. I. H., Redmill, A., & Michael, M. (1988). Mouse glucose-6phosphate isomerase and neuroleukin have identical 3' sequences. *Nature*, *332*(31), 455–456.

Fiocca, R., Necchi, V., Sommi, P., Ricci, V., Telford, J., Cover, T., & Solcia, E. (1999). Release of Helicobacter pylori vacuolating cytotoxin by both a specific secretion pathway and budding of outer membrane vesicles. uptake of released toxin and vesicles by gastric epithelium. *Journal of Pathology*, *188*, 220–226.

Flores-Díaz, M., Monturiol-Gross, L., Naylor, C., & Alape-Girón, A. (2016). Bacterial Sphingomyelinases and Phospholipases as Virulence Factors. *Microbiology and Molecular Biology Reviews*, *80*(3), 597–628. https://doi.org/10.1128/MMBR.00082-15.Address

Franco, L., Mario, S., Sergio, H., Juan, H., Josepantoni, C., Pons, P., … Querol, E. (2018). Multifunctional Proteins : Involvement in Human Diseases and Targets of Current Drugs. *The Protein Journal*. https://doi.org/10.1007/s10930-018-9790-x

Frankland, G. C., & Frankland, P. F. (1887). Studies on Some New Micro-Organisms Obtained from Air. *Philosophical Transactions of the Royal Society*, 257–287. https://doi.org/10.1098/rstb.1887.0011

Frenzel, E., Doll, V., Pauthner, M., Lücking, G., Scherer, S., & Ehling-Schulz, M. (2012). CodY orchestrates the expression of virulence determinants in emetic Bacillus cereus by impacting key regulatory circuits. *Molecular Microbiology*, *85*(1), 67–88. https://doi.org/10.1111/j.1365-2958.2012.08090.x

Frenzel, E., Kranzler, M., Stark, T., Hofmannn, T., & Ehling-Schulz, M. (2015). The Endospore-Forming Pathogen Bacillus cereus Exploits a Small Colony Variant-Based Diversification Strategy in Response to Aminoglyoside Exposure. *MBio*, *6*(6), 1–10. https://doi.org/10.1128/mBio.01172-15.Editor

Gewirtz, A. T., Navas, T. A., Lyons, S., Paul, J., Madara, J. L., & Godowski, P. J. (2001). Cutting Edge: Bacterial Flagellin Activates Basolaterally Expressed TLR5 to Induce Epithelial Proinflammatory Gene Expression. *The Journal of Immunology*, *167*, 1882–1885. https://doi.org/10.4049/jimmunol.167.4.1882

Gilmore, M. S., Cruz-rodz, A. L., Leimeister-Wächter, M., Kreft, J., & Goebel, W. (1989). A Bacillus cereus Cytolytic Determinant , Cereolysin AB , Which Comprises the Phospholipase C and Sphingomyelinase Genes : Nucleotide Sequence and Genetic Linkage. *Journal of Bacteriology*, *171*(2), 744–753.

Go, A. (2004). Ceramide-1-phosphate : a novel regulator of cell activation. *FEBS Journal*, *562*, 5–10. https://doi.org/10.1016/S0014-5793(04)00211-X

Gould, S. J. (2013). As we wait: coping with an imperfect nomenclature for extracellular vesicles. *Journal of Extracellular Vesicles*, *2*, 3–5.

Grab, D. J., & Philipp, M. T. (1996). Borrelia burgdorferi possesses a collagenolytic activity. *FEMS Microbiology Letters*, *144*, 39–45.

Granum, P. E., Sullivan, K. O., & Lund, T. (1999). The sequence of the non-haemolytic enterotoxin operon from Bacillus cereus 1. *FEMS Microbiology Letters*, *177*, 225–229.

Guinebretiere, M.-H., Auger, S., Galleron, N., Contzen, M., Sarrau, B. De, Buyser, M. De, … Sorokin, A. (2013). Bacillus cytotoxicus sp . nov . is a novel thermotolerant species of the Bacillus cereus Group occasionally associated with food poisoning. *International Journal of Systematic and Evolutionary Microbiology*, *63*, 31–40. https://doi.org/10.1099/ijs.0.030627-0

Gurung, M., Moon, D. C., Choi, C. W., Lee, J. H., Bae, Y. C., Kim, J., … Lee, J. C. (2011). Staphylococcus aureus Produces Membrane-Derived Vesicles That Induce Host Cell Death. *Plos One*, *6*(11), 1–8. https://doi.org/10.1371/journal.pone.0027958

Harrington, D. J. (1996). Bacterial Collagenases and Collagen-Degrading Enzymes and Their Potential Role in Human Disease. *Infection and Immunity*, *64*(6), 1885–1891.

Hayashi, F., Smith, K. D., Ozinsky, A., Hawn, T. R., Yi, E. C., Goodlett, D. R., … Aderem, A. (2001). The innate immune response to bacterial ¯ agellin is mediated by Toll-like receptor 5. *Nature*, *410*, 1099–1103.

Heilkenbrinker, U., Dietrich, R., Didier, A., Zhu, K., Lindbäck, T., Granum, P., & Märtlbauer, E. (2013). Complex Formation between NheB and NheC Is Necessary to Induce Cytotoxic Activity by the Three- Component Bacillus cereus Nhe Enterotoxin. *PLoS ONE*, *8*(4), 1–11. https://doi.org/10.1371/journal.pone.0063104

Helgason, E., Økstad, O. L. E. A., Caugant, D. A., Mock, L. E., Hegna, I. D. A., Johansen, H. A., & Fouet, A. (2000). Bacillus anthracis, Bacillus cereus and Bacillus thuringiensis - One Species on the Basis of Genetic Evidence. *Applied and Environmental Microbiology*, *66*(6), 2627–2630.

Helgason, E., Tourasse, N. J., Meisal, R., Caugant, D. A., & Kolsto, A. B. (2004). Multilocus sequence typing scheme for bacteria of the Bacilluscereus group. *Appl Environ Microbiol*, *70*(1), 191–201. https://doi.org/10.1128/AEM.70.1.191

Henderson, B., & Martin, A. (2011). Bacterial Virulence in the Moonlight : Multitasking Bacterial Moonlighting Proteins Are Virulence Determinants in Infectious Disease.

Infection and Immunity, *79*(9), 3476–3491. https://doi.org/10.1128/IAI.00179-11

Hessvik, N. P., Øverbye, A., Brech, A., Torgersen, M. L., Jakobsen, I. S., Sandvig, K., & Llorente, A. (2016). PIKfyve inhibition increases exosome release and induces secretory autophagy. *Cellular and Molecular Life Sciences*, *73*(24), 4717–4737. https://doi.org/10.1007/s00018-016-2309-8

Hidalgo, I., Raub, T., & Borchardt, R. (1989). Characterization of the Human Colon Carcinoma Cell Line (Caco-2) as a Model Permeability. *Gastroenterology*, *96*(3), 732–748.

Hong, S., Kim, M., Lee, E., Kim, J. H., Kim, Y., Jeon, S. G., … Kim, Y. (2011). Extracellular vesicles derived from Staphylococcus aureus induce atopic dermatitis-like skin inflammation. *Experimental Allergy and Immunology*, *66*(15), 351–359. https://doi.org/10.1111/j.1398-9995.2010.02483.x

Il, H., Hee, N., Yeon, S., Hyun, M., Hee, J., Hyun, S., … Chul, J. (2019). Microbial Pathogenesis Inhibitory e ff ects of thymol on the cytotoxicity and in fl ammatory responses induced by Staphylococcus aureus extracellular vesicles in cultured keratinocytes. *Microbial Pthogenesis*, *134*, 1–6. https://doi.org/10.1016/j.micpath.2019.103603

Järveläinen, H., Sainio, A., Koulu, M., Wight, T. N., & Penttinen, R. (2009). Extracellular Matrix Molecules : Potential Targets in Pharmacotherapy. *Pharmacological Reviews*, *61*(2), 198–223. https://doi.org/10.1124/pr.109.001289.provided

Jeffery, C. (2019). The Use of Proteomics Studis in Identifying Moonlighting Proteins. *Methods in Moleular Biology*, *1871*, 437–443.

Jernigan, D. B., Raghunathan, P. L., Bell, B. P., Brechner, R., Bresnitz, E. a, Butler, J. C., … Gerberding, J. L. (2002). Investigation of Bioterrorism- Related Anthrax, United States, 2001: Epidemiologic Findings. *Emerging Infectious Diseases*, *8*(10), 1019–1028. https://doi.org/10.3201/eid0810.020353

Jeßberger, N., Rademacher, C., Krey, V., Dietrich, R., Mohr, A.-K., Böhm, M.-E., … Märtlbauer, E. (2017). Simulating Intestinal Growth Conditions Enhances Toxin Production of Enteropathogenic Bacillus cereus. *Frontiers in Microbiology*, *8*(627), 1–15. https://doi.org/10.3389/fmicb.2017.00627

Jeßberger, N., Kranzler, M. *et al*. (in press)

Jiménez, G., Urdiain, M., Cifuentes, A., López-lópez, A., Blanch, A. R., Tamames, J., … Rosselló-móra, R. (2013). Description of Bacillus toyonensis sp . nov ., a novel species of the Bacillus cereus group , and pairwise genome comparisons of the species of the

group by means of ANI calculations. *Systematic and Applied Microbiology*, *36*, 383–391. https://doi.org/10.1016/j.syapm.2013.04.008

Katsu, M., Hama, Y., Utsumi, J., Takashina, K., Yasumatsu, H., Mori, F., … Sasaki, H. (2019). MicroRNA expression profiles of neuron-derived extracellular vesicles in plasma from patients with amyotrophif lateral sclerosis. *Neuroscience Letters*.

Keim, P., Price, L. B., Klevytska, A. M., Smith, K. L., Schupp, J. M., Okinaka, R., & Jackson, P. J. (2000). Multiple-Locus Variable-Number Tandem Repeat Analysis Reveals Genetic Relationships within Bacillus anthracis. *Journal of Bacteriology*, *182*(10), 2928–2936.

Koeppen, K., Hampton, T. H., Jarek, M., Scharfe, M., Gerber, A., Mielcarz, D. W., … Hammond, J. H. (2016). A Novel Mechanism of Host-Pathogen Interaction through sRNA in Bacterial Outer Membrane Vesicles. *PLOS Pathogens*, *12*(6), 1–22. https://doi.org/10.1371/journal.ppat.1005672

Kolesnick, R., & Golde, D. W. (1994). The Sphingomyelin Pathway in Tumor Necrosis Factor and Interleukin-1 Signaling. *Cell*, *77*, 325–326.

Kolstø, A., Tourasse, N. J., & Økstad, O. A. (2009). What Sets Bacillus anthracis Apart from Other Bacillus Species ? *Annual Review Microbiology*, *63*, 451–476. https://doi.org/10.1146/annurev.micro.091208.073255

Kramer, J. M., & Gilbert, R. J. (1989). Bacillus cereus and other Bacillus species. *Food-Borne Bacterial Pathogens.*, 21–70.

Kulp, A., & Kuehn, M. J. (2010). Biological Functions and Biogenesis of Secreted Bacterial Outer Membrane Vesicles. *Annual Review of Microbiology*, *64*(1), 163–184. https://doi.org/10.1146/annurev.micro.091208.073413

Lechner, S., Mayr, R., Francis, K. P., Pruss, B. M., Kaplan, T., Wiessner-Gunkel, E., … Scherer, S. (1998). Bacillus weihenstephanensis sp. nov. is a new psychrotolerant species of the Bacillus cereus group. *International Journal of Systematic Bacteriology*, *48*(4), 1373–1382. https://doi.org/10.1099/00207713-48-4-1373

Lee, Choi, C.-W., Lee, T., Kim, S. Il, Lee, J.-C., & Shin, J.-H. (2013). Transcription Factor σB Plays an Important Role in the Production of Extracellular Membrane-Derived Vesicles in Listeria monocytogenes. *PLoS ONE*, *8*(8), e73196. https://doi.org/10.1371/journal.pone.0073196

Lee, E., Choi, D., Kim, D., Kim, J., Park, J. O., Kim, S., … Gho, Y. S. (2009). Gram-positive bacteria produce membrane vesicles : Proteomics-based characterization of Staphylococcus aureus -derived membrane vesicles. *Proteomics*, *9*, 5425–5436.

https://doi.org/10.1002/pmic.200900338

Lee, J., Kim, S., Choi, D., Lee, J. S., & Kim, D. (2015). Proteomic analysis of extracellular vesicles derived from Mycobacterium tuberculosis. *Proteomics*, *15*, 3331–3337. https://doi.org/10.1002/pmic.201500037

Levi, M., & Cate, H. Ten. (1999). Disseminated Intravascular coagulation. *The New England Journal of Medicine*, *341*(8), 586–592.

Lindbäck, T., Fagerlund, A., Rødland, M. S., & Granum, P. E. (2004). Characterization of the Bacillus cereus Nhe enterotoxin. *Microbiology*, *150*, 3959–3967. https://doi.org/10.1099/mic.0.27359-0

Lindbäck, T., Hardy, S. P., Dietrich, R., Sødring, M., Didier, A., Moravek, M., … Ma, E. (2010). Cytotoxicity of the Bacillus cereus Nhe Enterotoxin Requires Specific Binding Order of Its Three Exoprotein Components . *Infection and Immunity*, *78*(9), 3813–3821. https://doi.org/10.1128/IAI.00247-10

Liu, Y., Defourny, K. A. Y., Smid, E. J., Abee, T., Capozzi, V., & Kim, S. Il. (2018). Gram-Positive Bacterial Extracellular Vesicles and Their Impact on Health and Disease. *Frontiers in Microbiology*, *9*(1502), 1–8. https://doi.org/10.3389/fmicb.2018.01502

Lund, T., Buyser, M. De, Einar, P., & Aliments, Â. S. (2000). A new cytotoxin from Bacillus cereus that may cause necrotic enteritis. *Molecular Microbiology*, *38*(2), 254–261.

Lund, T., & Granum, P. E. (1996). Characterisation of a non-haemolytic enterotoxin complex from Bacillus cereus isolated after a foodborne outbreak. *FEMS Microbiology Letters*, *141*, 151–156.

Lund, T., & Granum, P. E. (1999). The 105-kDa protein component of Bacillus cereus non-haemolytic enterotoxin (Nhe) is a metalloprotease with gelatinolytic and collagenolytic activity. *FEMS Microbiology Letters*, *178*, 355–361.

Macnab, R. M. (1992). Genetics and biogenesis of bacterial flagella. *Ann. Rev. Genet.*, *26*, 131–158.

Martin, S. F., Follows, B. C., Hergenrother, P. J., & Trotter, B. K. (2000). The Choline Binding Site of Phospholipase C (Bacillus cereus): Insights into Substrate Specificity. *Biochemistry*, *39*, 3410–3415.

Matsushita, O., Yoshihara, K., & Katayama, S. (1994). Purification and Characterization of a Clostridium perfringens 120-Kilodalton Collagenase and Nucleotide Sequence of the Corresponding Gene. *Journal of Bacteriology*, *176*(1), 149–156.

Mazzantini, D., Celandroni, F., Salvetti, S., Gueye, S. A., Lupetti, A., Senesi, S., & Ghelardi, E. (2016). FlhF Is Required for Swarming Motility and Full Pathogenicity of Bacillus

cereus. *Frontiers in Microbiology*, *7*, 1–9. https://doi.org/10.3389/fmicb.2016.01644

Mcbroom, A. J., Johnson, A. P., Vemulapalli, S., & Kuehn, M. J. (2006). Outer Membrane Vesicle Production by Escherichia coli Is Independent of Membrane Instability. *Journal of Bacteriology*, *188*(15), 5385–5392. https://doi.org/10.1128/JB.00498-06

Messelhäußer, U., & Ehling-Schulz, M. (2018). Bacillus cereus—a Multifaceted Opportunistic Pathogen. *Current Clinical Microbiology Reports*, *5*(2), 120–125. https://doi.org/10.1007/s40588-018-0095-9

Mock, M., & Fouet, A. (2001). Anthrax. *Annual Review of Microbiology*, *55*, 647–671.

Moravek, M., Dietrich, R., & Buerk, C. (2006). Determination of the toxic potential of Bacillus cereus isolates by quantitative enterotoxin analyses. *FEMS Microbiology Letters*, *257*, 293–257. https://doi.org/10.1111/j.1574-6968.2006.00185.x

Mukherjee, S., & Kearns, D. B. (2014). The structure and regulation of flagella in Bacillus subtilis. *Annual Review of Genetics*, *48*, 319–340. https://doi.org/10.1146/annurev-genet-120213-092406.The

Muzzi, A., Masignani, V., & Rappuoli, R. (2007). The pan-genome : towards a knowledge-based discovery of novel targets for vaccines and antibacterials. *Drug Discovery Today*, *12*(11/12), 429–439. https://doi.org/10.1016/j.drudis.2007.04.008

Nakamura, L. K., & Jackson, M. A. (1995). Clarification of the Taxonomy of Bacillus mycoides. *International Journal of Systematic Bacteriology*, *45*(1), 46–49.

Naranjo, M., Denayer, S., Botteldoorn, N., Delbrassinne, L., Veys, J., Waegenaere, J., … Dierick, K. (2011). Sudden Death of a Young Adult Associated with Bacillus cereus Food Poisoning . *Journal of Clinical Microbiology*, *49*(12), 4379–4381. https://doi.org/10.1128/JCM.05129-11

Neuhaus, F. C., & Baddiley, J. (2003). A Continuum of Anionic Charge: Structures and Functions of D- Alanyl- Teichoic Acids in Gram- Positive Bacteria. *Microbiology and Molecular Biology Reviews*, *67*(4), 686. https://doi.org/10.1128/MMBR.67.4.686

Oda, M., Fujita, A., Okui, K., Miyamoto, K., Shibutani, M., & Takagishi, T. (2013). Biochemical and Biophysical Research Communications Bacillus cereus sphingomyelinase recognizes ganglioside GM3. *Biochemical and Biophysical Research Communications*, *431*(2), 164–168. https://doi.org/10.1016/j.bbrc.2013.01.002

Oda, M., Hashimoto, M., Takahashi, M., Ohmae, Y., Seike, S., Kato, R., … Sakurai, J. (2012). Role of Sphingomyelinase in Infectious Diseases Caused by Bacillus cereus. *PLoS ONE*, *7*(6), 1–11. https://doi.org/10.1371/journal.pone.0038054

Oliveira, D. L., Nakayasu, E. S., Joffe, L. S., Guimarães, A. J., Sobreira, T. J. P., Nosanchuk,

J. D., … Rodrigues, M. L. (2010). Biogenesis of extracellular vesicles in yeast. *Communicative & Integrative Biology*, *3*(6), 533–535. https://doi.org/10.4161/cib.3.6.12756

Ollinger, J., Bowen, B., Wiedmann, M., Boor, K. J., & Bergholz, T. M. (2009). Listeria monocytogenes ??B modulates PrfA-mediated virulence factor expression. *Infection and Immunity*, *77*(5), 2113–2124. https://doi.org/10.1128/IAI.01205-08

Openshaw, A. E. A., Race, P. R., Monzo, H. J., Vazquez-Boland, J.-A., & Banfield, M. J. (2005). Crystal Structure of SmcL , a Bacterial Neutral Sphingomyelinase C from Listeria *. *Journal of Biological Chemistry*, *280*(41), 35011–35017. https://doi.org/10.1074/jbc.M506800200

Pomerantsev, A. P., Kalnin, K. V, Osorio, M., & Leppla, S. H. (2003). Phosphatidylcholine-Specific Phospholipase C and Sphingomyelinase Activities in Bacteria of the Bacillus cereus Group. *Infection and Immunity*, *71*(11), 6591–6606. https://doi.org/10.1128/IAI.71.11.6591

Prados-Rosales, R., Baena, A., Martinez, L. R., Luque-garcia, J., Kalscheuer, R., Veeraraghavan, U., … Casadevall, A. (2011). Mycobacteria release active membrane vesicles that modulate immune responses in a TLR2-dependent manner in mice. *The Journal of Clinical Investigation*, *121*(4), 1471–1483. https://doi.org/10.1172/JCI44261.disease

Proctor, R. A., Eiff, C. Von, Kahl, B. C., Becker, K., Mcnamara, P., Herrmann, M., & Peters, G. (2006). Small colony variants : a pathogenic form of bacteria that facilitates persistent and recurrent infections. *Nature Reviews Microbiology*, *4*, 295–305. https://doi.org/10.1038/nrmicro1384

Raivio, T. L. (2005). Envelope stress responses and Gram-negative bacterial pathogenesis. *Molecular Microbiology*, *56*(5), 1119–1128. https://doi.org/10.1111/j.1365-2958.2005.04625.x

Ramarao, N., Nielsen-leroux, C., & Lereclus, D. (2012). The Insect Galleria mellonella as a Powerful Infection Model to Investigate Bacterial Pathogenesis. *Journal of Visualized Experiments*, *70*, 1–7. https://doi.org/10.3791/4392

Ravnum, S., Økstad, O. A., Gohar, M., Faegri, K., Kolstø, A., & Lereclus, D. (2008). The PlcR Virulence Regulon of Bacillus cereus. *PLoS ONE*, *3*(7), 1–9. https://doi.org/10.1371/journal.pone.0002793

Read, J., Pearce, J., Li, X., Muirhead, H., Chirgwin, J., & Davies, C. (2001). The Crystal Structure of Human Phosphoglucose Ê Resolution : Implications for Isomerase at 1 . 6 A Catalytic Mechanism , Cytokine Activity and Haemolytic Anaemia. *Journal of Molecular*

Biology, *309*, 447–463. https://doi.org/10.1006/jmbi.2001.4680

Read, T. D., Peterson, S. N., & Tourasse, N. (2003). The genome sequence of Bacillus anthracis Ames and comparison to closely related bacteria. *Natu*, *423*, 81–86. https://doi.org/10.1038/nature01590.1.

Rivera, J., Cordero, R. J. B., Nakouzi, A. S., Frases, S., & Nicola, A. (2010). Bacillus anthracis produces membrane-derived vesicles containing biologically active toxins. *PNAS*, *107*(44), 19002–19007. https://doi.org/10.1073/pnas.1008843107/-/DCSupplemental.www.pnas.org/cgi/doi/10.1073/pnas.1008843107

Rodrigues, M. L., Nakayasu, E. S., Oliveira, D. L., Nimrichter, L., Nosanchuk, J. D., Almeida, I. C., & Casadevall, A. (2008). Extracellular vesicles produced by Cryptococcus neoformans contain protein components associated with virulence. *Eukaryotic Cell*, *7*(1), 58–67. https://doi.org/10.1128/EC.00370-07

Roier, S., Zingl, F., Durakovic, S., Kohl, P., Eichmann, T., Klug, L., … Schild, S. (2015). A novel mechanism for the biogenesis of outer membrane vesicles in Gram-negative bacteria. *Nature Communications*, *7*(10515), 1–13.

Rolhion, N., Barnich, N., Claret, L., & Darfeuille-michaud, A. (2005). Strong Decrease in Invasive Ability and Outer Membrane Vesicle Release in Crohn ' s Disease-Associated Adherent-Invasive Escherichia coli Strain LF82 with the yfgL Gene Deleted. *Jour*, *187*(7), 2286–2296. https://doi.org/10.1128/JB.187.7.2286

Ruggiero, M. A., Gordon, D. P., Orrell, T. M., Bailly, N., Bourgoin, T., Brusca, R. C., … Kirk, M. (2015). A Higher Level Classification of All Living Organisms. *PLoS ONE*, *10*(4), 1–60. https://doi.org/10.1371/journal.pone.0119248

Rutter, B. D., & Innes, R. W. (2017). Extracellular Vesicles Isolated from the Leaf Apoplast. *Plant Physiology*, *173*, 728–741. https://doi.org/10.1104/pp.16.01253

Salamitou, S., Francoise, R., Brehelin, M., Bourguet, D., Gilois, N., Gominet, M., … Lereclus, D. (2000). The plcR regulon is involved in the opportunistic properties of Bacillus thuringiensis and Bacillus cereus in mice and insects. *Microbiology*, (146), 2825–2832.

Schaefer, L., & Schaefer, R. M. (2010). Proteoglycans : from structural compounds to signaling molecules. *Cell Tissue Research*, *339*, 237–246. https://doi.org/10.1007/s00441-009-0821-y

Schlatterer, K., Beck, C., Hanzelmann, D., Lebtig, M., Fehrenbacher, B., Schallter, M., … Peschel, A. (2018). crossm The Mechanism behind Bacterial Lipoprotein Release : Phenol- Extracellular Vesicle Release from Staphylococcus aureus. *Katja Schlatterer,a Christian Beck,a Dennis Hanzelmann,a Marco Lebtig,a Birgit Fehrenbacher,b Martin*

Schaller,b Patrick Ebner,c Mulugeta Nega,c Michael Otto,d Dorothee Kretschmer,a Andreas Peschela, *9*(6), 1–13.

Schneider, C. A., Rasband, W. S., & Eliceiri, K. W. (2012). HISTORICAL commentary NIH Image to ImageJ : 25 years of image analysis. *Nature Methods*, *9*(7), 671–675. https://doi.org/10.1038/nmeth.2089

Schrempf, H., Koebsch, I., Walter, S., Engelhardt, H., & Meschke, H. (2011). Extracellular Streptomyces vesicles : amphorae for. *Microbial Biotechnology*, *4*(2), 286–299. https://doi.org/10.1111/j.1751-7915.2011.00251.x

Sela, S., Schickler, H., Chet, I., & Spiegel, Y. (1998). Purification and characterization of a B acillus cereus collagenolytic / proteolytic enzyme and its effect on Meloidogyne javanica cuticular proteins. *European Journal of Plant Pathology*, *104*, 59–60.

Sharom, F. J., & Lehto, M. T. (2002). Glycosylphosphatidylinositol-anchored proteins : structure , function , and cleavage by phosphatidylinositol-specific phospholipase C. *Biochemistry and Cell Biology*, *549*, 535–549. https://doi.org/10.1139/O02-146

Silhavy, T. J., Kahne, D., & Walker, S. (2010). The Bacterial Cell Envelope. *Cold Spring Harbor Perpectives in Biology*, 1–16. https://doi.org/10.1101/cshperspect.a000414

Silverman, J. M., Clos, J., Oliveira, C. C. De, Shirvani, O., Fang, Y., Wang, C., … Reiner, N. E. (2010). An exosome-based secretion pathway is responsible for protein export from Leishmania and communication with macrophages. *Journal of Cell Scien*, 842–852. https://doi.org/10.1242/jcs.056465

Sjöström, A. E., Sandblad, L., Uhlin, B. E., & Wai, S. N. (2015). Membrane vesicle-mediated release of bacterial RNA. *Scientific Reports*, *5*(153299), 1–10. https://doi.org/10.1038/srep15329

Slamti, L., & Lereclus, D. (2002). A cell ± cell signaling peptide activates the PlcR virulence regulon in bacteria of the Bacillus cereus group. *Embo J.*, *21*(17), 4550–4559.

Slein, M. W., & Logan, G. F. (1965). Characterization of the Phospholipases of Bacillus cereus and Their Effects on Erythrocytes , Bone , and Kidney Cells. *Journal of Bacteriology*, *90*(I), 69–81.

Stenfors Arnesen, L. P., Fagerlund, A., & Granum, P. E. (2008). From soil to gut: Bacillus cereus and its food poisoning toxins. *FEMS Microbiology Reviews*, *32*(4), 579–606. https://doi.org/10.1111/j.1574-6976.2008.00112.x

Takeo, K., Uesaka, I., Uehira, K., & Nishiura, M. (1973). Fine structure of Cryptococcus neoformans grown in vitro as observed by freeze-etching. *Journal of Bacteriology*, *113*(3), 1442–1448.

Tartaglia, N. R., Breyne, K., Meyer, E., Cauty, C., Jardin, J., & Alonzo, F. (2018). Staphylococcus aureus Extracellular Vesicles Elicit an Immunostimulatory Response in vivo on the Murine Mammary Gland. *Frontiers in Cellular and Infection Microbiology*, *8*(277), 1–17. https://doi.org/10.3389/fcimb.2018.00277

Theocharis, A. D., Skandalis, S. S., Gialeli, C., & Karamanos, N. K. (2015). Extracelllular Matrix Structure. *Advanced Drug Delivery Reviews*, 1–76. https://doi.org/10.1016/j.addr.2015.11.001

Théry, C., Witwer, K. W., Aikawa, E., Alcaraz, M. J., Anderson, J. D., Andriantsitohaina, R., … Lowry, M. C. (2018). Minimal information for studies of extracellular vesicles 2018 (MISEV2018): a position statement of the International Society for Extracellular Vesicles and update of the MISEV2014 guidelines. *Journal of Extracellular Vesicles*, *3078*. https://doi.org/10.1080/20013078.2018.1535750

Titball, R. W. (1993). Bacterial Phospholipases C. *Microbiological Reviews*, *57*(2), 347–366.

Tkach, M., & Thery, C. (2016). Review Communication by Extracellular Vesicles : Where We Are and Where We Need to Go. *Cell*, *164*, 1226–1232. https://doi.org/10.1016/j.cell.2016.01.043

Toyofuku, M., Nomura, N., & Eberl, L. (2019). Types and origins of bacterial membrane vesicles. *Nature Reviews Microbiology*, *17*, 13–24. https://doi.org/10.1038/s41579-018-0112-2

Vallejo, M. C., Nakayasu, E. S., Longo, L. V. G., Ganiko, L., Lopes, F. G., Matsuo, A. L., … Puccia, R. (2012). Lipidomic analysis of extracellular vesicles from the pathogenic phase of Paracoccidioides brasiliensis. *PLoS ONE*, *7*(6), 1–10. https://doi.org/10.1371/journal.pone.0039463

Wai, S. N., Takede, A., & Amako, K. (1995). The Release of Outer Membrane Vesicles from Strains of Enterotoxigenic Escherichia coli. *Microbiology and Immunology*, *39*(7), 451–456.

Wan, L., Meng, D., Wang, H., Wan, S., Jiang, S., Huang, S., … Yu, P. (2017). Preventive and Therapeutic Effects of Thymol in a Lipopolysaccharide-Induced Acute Lung Injury Mice Model. *Inflammation*. https://doi.org/10.1007/s10753-017-0676-4

Wang, E., Liu, Y., Qiu, X., Tang, Y., Wang, H., & Xiao, X. (2019). Bacteria-released outer membrane vesicles promote disseminated intravascular coagulation. *Thrombosis Research*, *178*(November 2018), 26–33. https://doi.org/10.1016/j.thromres.2019.03.019

Wang, Q., Suzuki, A., Mariconda, S., Porwollik, S., & Harshey, R. M. (2005). Sensing wetness : a new role for the bacterial flagellum. *Embo J.*, *24*, 2034–2042.

https://doi.org/10.1038/sj.emboj.7600668

Wang, X., Thompson, C. D., Weidenmaier, C., & Lee, J. C. (2018). Release of Staphylococcus aureus extracellular vesicles and their application as a vaccine platform. *Nature Communications*, *9*(1379). https://doi.org/10.1038/s41467-018-03847-z

Wolffian, T., & Conn, M. (1938). The flagellation of bacteria. *Science*, (258), 283–284.

Work, E., Knox, K. W., & Vesk, M. (1966). The Chemistry and Electron microscopy of an Extracelular Lipopolysaccharide from Escherichia Coli. *Ann. N. Y Acad. Sci.*, *133*, 438–449.

Wright, S. D., & Kolesnick, R. N. (1995). Does endotoxin stimulate cells by mimicking ceramide ? *Immunology Today*, *16*(6), 297–302.

Yamamoto, Y., Harashima, A., Saito, H., Munesue, S., Motoyoshi, S., Han, D., … Alerts, E. (2019). Septic Shock Is Associated with Receptor for Advanced Glycation End Products Ligation of LPS. *The Journal of Immunology*, *186*, 3248–3257. https://doi.org/10.4049/jimmunol.1002253

Yanlong, J., Qingke, K., Kenneth, L. R., & Roy, C. I. (2014). Membrane vesicles of Clostridium perfringens Type A strains induce innate and adaptive immunity. *Int J Med Microbiol*, *304*, 431–443. https://doi.org/10.1016/j.ijmm.2014.02.006.Membrane

Zenewicz, L. A., Wei, Z., Goldfine, H., & Shen, H. (2005). Phosphatidylinositol-specific Phospholipase C of Bacillus anthracis Down-Modulates the Immune Response. *Journnal of Immunology*, *174*, 8011–8016. https://doi.org/10.4049/jimmunol.174.12.8011